Vapor–Liquid Equilibrium of Ethyl Lactate Highly Diluted in Ethanol–Water Mixtures at 101.3 kPa. Experimental Measurements and Thermodynamic Modeling Using Semiempirical Models

Cristian Puentes, Xavier Joulia, Patrice Paricaud, Pierre Giampaoli, Violaine Athès, Martine Esteban-Decloux

Vapor–Liquid Equilibrium of Ethyl Lactate Highly Diluted in Ethanol–Water Mixtures at 101.3 kPa. Experimental Measurements and Thermodynamic Modeling Using Semiempirical Models

Cristian Puentes,[†] Xavier Joulia,[‡] Patrice Paricaud,[§] Pierre Giampaoli,[†] Violaine Athès,[⊥] and Martine Esteban-Decloux*[,†]

[†]Unité Mixte de Recherche Ingénierie Procédés Aliments, AgroParisTech, INRA, Université Paris-Saclay, F-91300 Massy, France

[‡]Laboratoire de Génie Chimique, Université de Toulouse INPT-ENSIACET, CNRS, F-31030 Toulouse, France

[§]Unité de Chimie et Procédés, ENSTA ParisTech, Université Paris-Saclay, F-91762 Palaiseau, France

[⊥]Unité Mixte de Recherche Génie et Microbiologie des Procédés Alimentaires, AgroParisTech, INRA, Université Paris-Saclay, F-78850 Thiverval-Grignon, France

S *Supporting Information*

ABSTRACT: A thermodynamic study of the vapor–liquid equilibrium for the ternary system ethyl lactate–ethanol–water was performed at 101.3 kPa and infinite dilution regarding ethyl lactate, for boiling temperatures ranging from (352.3 to 370.0) K. The experimental measurements were carried out with a recirculation still and the equilibrium compositions of ethyl lactate were determined by gas chromatography. The volatility of ethyl lactate decreases when the ethanol content in the liquid phase is increased. The investigated system was correctly correlated by the NRTL and UNIQUAC models, with an average absolute relative deviation below 10%. The comparison with the results obtained from interaction parameters fitted to experimental data of the binary systems ethyl lactate–ethanol and ethyl lactate–water at 101.3 kPa, proves that the parameters calculated in this work give a better description of the ethyl lactate volatility, a key parameter in distillation, at low concentrations. These latter parameters are therefore recommended for process simulation and optimization in alcoholic beverages production.

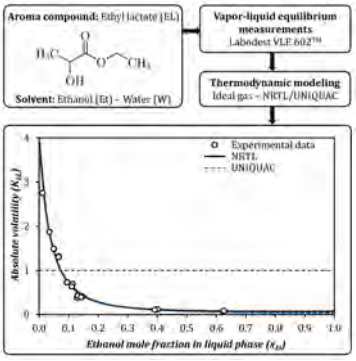

INTRODUCTION

Process simulation is a powerful tool to design, analyze, and optimize chemical and biochemical processes. For the correct simulation of separation units, there are two factors of crucial importance: (1) a reliable and accurate knowledge of the phase equilibria, and (2) a suitable choice of thermodynamic models to correctly describe the volumetric behavior of the involved phases.[1−7]

In alcoholic distillation, some simulation studies have been performed over the last 50 years with the aim of identifying and predicting the influence of operating parameters on process variables such as product quality and efficiency.[6,7] These researches have been focused on continuous processes for the production of whisky,[8] neutral alcohol,[6,7,9] bioethanol,[10−12] cachaça,[13] and anhydrous fuel ethanol.[14] In batch distillation, simulation has been applied for the analysis of the recovery process of ethanol produced from banana culture waste,[15] as well as the production of pisco,[16,17] cachaça in a lab-scale pot still,[18,19] whisky,[7] pear distillates,[20] and bitter orange distillates.[6] The simulations were performed by either implementing mathematical models of mass and energy balances or using commercial software as AspenPlus, Aspen Dynamics, BatchColumn, ChemCAD, Pro/II, and ProSimPlus.

The common point among these studies is that the feedstock was modeled as a simplified mixture of ethanol and water with several minor volatile species, known as congeners or aroma compounds. The number of aroma compounds considered varies between 0 and 16 and the chemical families included are acetals (acetal), alcohols (methanol, propan-1-ol, propan-2-ol, 2-propen-1-ol, 2-methylpropan-1-ol, butan-1-ol, butan-2-ol, 2-methylbutan-1-ol, 3-methylbutan-1-ol, pentan-1-ol, pentan-2-ol, hexan-1-ol, 2-phenylethanol), carbonyl compounds (acetaldehyde, acetone), carboxylic acids (acetic acid, propionic acid, octanoic acid), esters (methyl acetate, ethyl acetate, ethyl hexanoate, ethyl decanoate), furanes (furfural), and terpenes (pinene, limonene, linalool, linalool oxide). Carbon dioxide has also been considered in some researches, in order to analyze its influence on the product composition.[7,10,11,14]

In alcoholic beverages production, the understanding of aroma compounds behavior in distillation is fundamental since they are responsible for the product quality. Several hundred of aroma compounds are mainly generated at low concentrations during the fermentation step and a lower proportion during distillation

DOI: 10.1021/acs.jced.7b00770

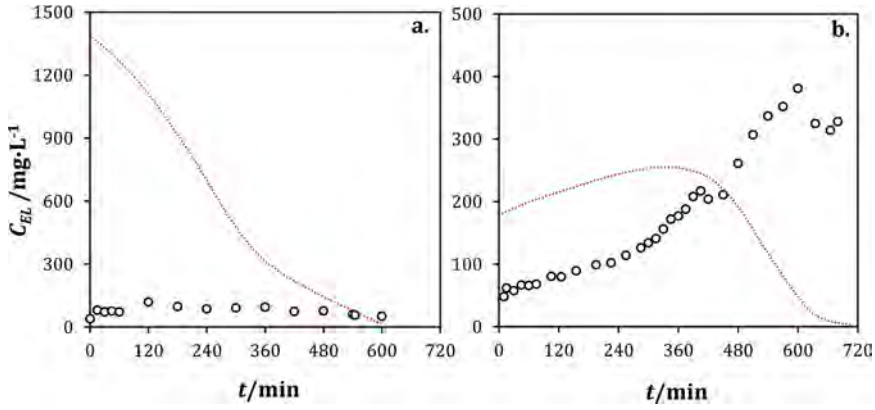

Figure 1. Evolution of the ethyl lactate concentration (C_{EL}) in the distillate at 20 °C over time (t) during the (a) first batch distillation and (b) second batch distillation. (○) Experimental data from Cantagrel et al.[34] (···) Simulation using UNIFAC 1993 and the ideal gas equation.

and maturation.[21−26] The simulation studies from the literature have included some of the most representative species. However, other important aroma compounds, such as ethyl lactate, have never been analyzed.

Ethyl 2-hydroxypropanoate, commonly known as ethyl lactate, is produced by the reaction of lactic acid, from malolactic fermentation, with ethanol. This compound has been quantified in wine and distilled beverages at very different concentration levels. In wine from traces to 500 mg·L^{-1} and in distillates up to 400 mg·L^{-1}.[27−29] Together with ethyl acetate, they constitute the main esters found in distillates.[30] From a sensory point of view, ethyl lactate may act as a stabilizer of the distillate flavor as well as a softener of the harsh flavor characteristics if it is present at low concentrations. However, at higher concentration levels, caused by lactic acid bacteria spoilage, this compound deteriorates the organoleptic quality of distillates.[28,30] In this case, process simulation may represent a useful tool to predict and control the concentration of this aroma compound to the desired levels.

As part of a confidential study carried out in our research group about cognac distillation,[31] the composition profiles of ethanol and 23 aroma compounds, including ethyl lactate, were simulated using the commercial software BatchColumn provided by ProSim. The thermodynamic models chosen for the representation of the vapor and liquid phases were respectively the ideal gas equation and the predictive model UNIFAC 1993.[32,33] According to Figure 1, in which simulation is compared to validated experimental data from a distillation campaign at atmospheric pressure,[34] the temporal evolution of ethyl lactate concentration in the distillate is not at all well represented during the two series batch distillations of the traditional process, known as Charentaise distillation. In the first distillation, Figure 1a, the concentration is highly overestimated and follows a strongly decreasing trend, against a rather constant path of the experimental data. In the second one, Figure 1b, the composition profile has a maximum in the middle of the distillation period, whereas the experimental data follow an increasing trend before the depletion of ethyl lactate in the boiler, toward the end of the operation. From these experimental data, one can conclude that ethyl lactate is mainly found in the tails fraction (last cut of the second distillation), even if it is also present in the core distillate fractions, and that its volatility is therefore presumably low.

In this context, the knowledge of vapor−liquid equilibrium data of this aroma compound and a better thermodynamic model choice are indispensable to correctly describe and predict its behavior in distillation. To our knowledge vapor−liquid equilibrium data for ethyl lactate highly diluted in ethanol−water mixtures at 101.3 kPa have not been reported in the literature. Only binary equilibrium data have been generated: (1) at isobaric conditions for the ethyl lactate (EL)−ethanol (Et) system at 101.3 kPa[35] and (2) isothermal conditions for the ethyl lactate (EL)−ethanol (Et) system (at 313.15, 333.25, and 353.35 K) and for the ethyl lactate (EL)−water (W) system (at 313.15 K, 333.15 K).[36] Isobaric equilibrium data for the ethyl lactate (EL)−lactic acid (LA)−ethanol (Et)−water (W) quaternary system at 101.3 kPa has also been reported.[37] For the binary measurements, the whole liquid composition range of ethyl lactate was considered, x_{EL} = (0 to 1) mole fraction, whereas for the quaternary system, the interval is more reduced, x_{EL} = (0.02 to 0.20) mole fraction. In both cases the number of experimental data in the vicinity of x_{EL} = 0 is very reduced. Concerning the ternary mixture ethyl lactate−ethanol−water, only experimental distillation data are available, including those presented in Figure 1 for cognac distillation[34] and some composition profiles of ethyl lactate concentration in the distillate as a function of the ethanol volume fraction in armagnac distillation.[38]

The objective of this work is thus to generate experimental vapor−liquid equilibrium data of ethyl lactate highly diluted over a composition range of the ethanol−water solution corresponding to a temperature interval from (352.3 to 370.0) K at 101.3 kPa. The equilibrium measurements are performed with a recirculation Gillespie-like still,[39] a device based on a dynamic method recommended in the literature for measurements at temperatures higher than 298.15 K. This procedure provides a direct and simple way to determine the equilibrium behavior of dilute mixtures, when coupled to an accurate quantitative analysis of the liquid and condensed vapor composition[40,41] and has been used to estimate activity coefficients of methanol and ethanol highly diluted in water[40] as well as partition coefficients of aroma compounds in hydroalcoholic mixtures.[42,43] In both cases, the results proved to be consistent with respect to distillation data and model correlation.

The equilibrium data are then correlated with the NRTL and UNIQUAC models in order to determine the interaction parameters required in process simulators for the simulation of the ethyl lactate composition profiles in both continuous and discontinuous distillation of alcoholic beverages. These models have been used to correlate with satisfactory results the equilibrium data for ethanol−water system[44] as well as some

Table 1. Some Properties of the Compounds Studied in This Work

compound	CAS	molecular formula	MM/g·mol^{-1}	T_b/K[b]	supplier	supplier purity % mass	experimental purity[c]
(*R*,*S*)-ethyl 2-hydroxypropanoate[a]	97-64-3	$C_5H_{10}O_3$	118.31	427.65	Sigma-Aldrich (Saint-Quentin Fallavier, France)	≥98.00%	99.81%
ethanol	64-17-5	C_2H_6O	46.07	351.44	Carlo Erba (Val de Reuil, France)	≥99.90%	99.98%
water	7732-18-5	H_2O	18.01	373.15			

[a]A racemic mixture of L- and D-enantiomers, thereafter designed as ethyl lactate. [b]Riddick et al.[70] [c]This experimental volatile purity was calculated as the ratio between the surface area of the gas chromatographic peak associated to the chemical compound and the total area of all peaks detected. MM is the molar mass and T_b the boiling point at 101.3 kPa.

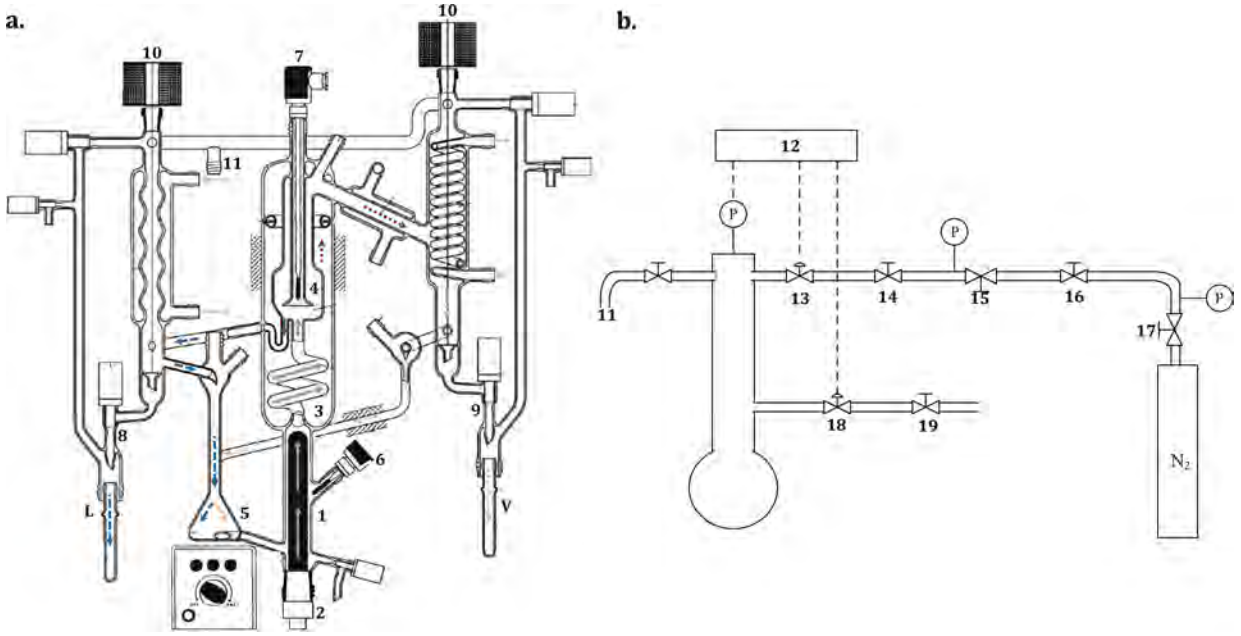

Figure 2. (a) Schema of the Labodest VLE 602. Adapted from Dias et al.[49] (b) Schema of the pressure control system. (1) Boiler, (2) Electrical resistance, (3) Contact path, (4) Separation chamber, (5) Mixing chamber, (6) Pt100 liquid probe, (7) Pt100 vapor probe, (8) Liquid sample port, (9) Vapor sample port, (10), Solenoid valves, (11) connection to the pressure control system, (12) control center, (13) solenoid valve $V_{N2\text{-}auto}$, (14) manual needle valve $V_{N2\text{-}man}$, (15) expansion valve, (16) on−off valve, (17) expansion valve, (18) solenoid valve $V_{Vent\text{-}auto}$, (19) manual needle valve $V_{Vent\text{-}amn}$. (dark gray solid arrow) vapor−liquid, (blue dashed arrow) liquid (L), (red dotted arrow) vapor (V), (pink dotted arrow) condensed vapor, (light gray solid arrow) refrigerant.

binary (aroma compound−ethanol and aroma compound water)[35,36,45,46] and multicomponent aroma systems.[42,43,47]

EXPERIMENTAL STUDY

Materials. The chemical compounds studied in this work are listed in Table 1, which includes the suppliers and some of their physicochemical properties. Deionized water was obtained using a Milli-Q system (Millipore waters. Molsheim, France). Concerning the total volatile compounds content, a supplementary purity test for ethyl lactate and ethanol was performed by gas chromatography with flame ionization detection (GC-FID). No further purification of both compounds was needed since their experimental purities were estimated to be higher than 99.8%.

The initial ternary mixtures for equilibrium measurements were prepared by precisely weighing known quantities of the three compounds. Because of the important quantity required for each equilibrium measurement (85 mL per ternary mixture, without considering the mixing flask mass), two weighing scales were used: one for ethyl lactate with an accuracy of ±0.0001 g and a maximum capacity of 100 g (Mettler AE240S weighing scale. L.P. Pesage. Angervilliers, France), and another for ethanol and water with an accuracy of ±0.01 g and a maximum capacity of 1000 g (Sartorious A2612. L.P. Pesage. Angervilliers, France).

Seventeen solutions with initial ethanol mass fractions ranging from $z_{mEt} = (6.2 \times 10^{-2}$ to $9.1 \times 10^{-1})$ (or in mole fractions $z_{Et} = (2.5 \times 10^{-2}$ to $8.0 \times 10^{-1})$) were independently brought into equilibrium. The concentration of ethyl lactate was fixed in every initial solution to $x_{mEL} = 1.0 \times 10^{-3}$, which corresponds to a mole composition interval $x_{EL} = (1.4 \times 10^{-4}$ to $3.5 \times 10^{-4})$.

Measurements of Vapor−Liquid Equilibrium. Vapor−liquid equilibrium measurements were carried out by using the apparatus Labodest VLE 602 (i-Fischer Engineering GmbH. Waldbüttelbrunn, Germany), an all-glass still of the Gillespie type based on a dynamic method at adiabatic and isobaric conditions, with recirculation of both liquid and vapor phases.

This equipment, Figure 2, has been previously used in our laboratory to measure vapor−liquid equilibria data for other aroma compounds.[42,43] A detailed description has been already reported.[42,48,49] Some elements are recalled below.

Each ternary mixture (a charge of 85 mL) is heated and partially evaporated in the boiler. The rising vapor, carrying fine boiling droplets, goes through a contact path and arrives to a chamber where phase separation takes place, owing to a reduction of the flow velocity. Both phases, liquid and vapor

(after condensation), circulate separately back to a mixing chamber connected to the boiler until thermodynamic equilibrium is reached. They are finally sampled for chromatographic analysis.

Two parameters were considered to ensure the equilibrium state: temperature, governed by the binary system ethanol−water (components in largest proportion), and composition. The time needed to reach a stable temperature (with a maximal standard uncertainty of ±0.3 K) was 30 min, whereas the time to reach composition equilibrium for this ternary system was determined by gas chromatography analysis to be about 2 h, once the temperature was constant.

The equilibrium temperature was measured by means of two Pt100 platinum probes (accuracy of ±0.05 K. i-Fischer Engineering GmbH. Waldbüttelbrunn, Germany), periodically calibrated against a reference platinum resistance thermometer (Pt100 Testo 735, accuracy of ±0.05 K; GFF. Chilly-Mazarin, France). To promote a continuous and smooth evaporation of the mixtures, the heating power was adjusted in such a way that the condensed vapor rate was 2 drops·s^{-1}.

Concerning the total pressure, it was monitored using a digital manometer (P-10 WIKA, accuracy of ± 0.1 kPa. i-Fischer Engineering GmbH. Waldbüttelbrunn, Germany) and controlled to the desired value with an electronic pressure controller (i-Fischer Engineering GmbH. Waldbüttelbrunn, Germany). This controller, presented in Figure 2 is composed of a pressurizing circuit with dry nitrogen and a venting circuit. The nitrogen circuit is used to increase the pressure, and comprises an expansion valve at the outlet of the storage bottle (where the pressure is set around 100 to 200 kPa), an on−off valve close to Labodest, a second expansion valve (for adjusting the pressure to 50 kPa maximum), a manual needle valve ($V_{N2\text{-}man}$) to vary the intake flow, and finally a solenoid valve ($V_{N2\text{-}auto}$) activated by the control center. A decrease of pressure is achieved by the activation of the vent valve ($V_{Vent\text{-}auto}$) and the adjustment of this leakage by the manual valve needle ($V_{Vent\text{-}man}$). In this study, the set point was maintained at 101.3 kPa with a maximal standard uncertainty of ± 0.5 kPa.

Determination of Equilibrium Compositions. *Ethyl Lactate Mass Fractions.* The analysis of ethyl lactate in the coexistent liquid and condensed vapor phases was performed by gas chromatography at the UNGDA laboratory. The equipment, a chromatograph 5890 series II, Hewlett-Packard (Agilent Technologies. Ulis, France) was coupled to a flame ionization detector (T = 220 °C, H_2, 40 mL·min^{-1}; air, 450 mL·min^{-1}; make-up gas He, 45 mL·min^{-1}. Agilent Technologies. Ulis, France). A polar, polyethylene glycol capillary column (DB-WAX. 60 m linear length, 0.50 mm internal diameter, 0.25 μm film thickness. Agilent Technologies. Ulis, France) was used as stationary phase for the analysis. Hydrogen was used as the carrier gas at constant flow rate of 2.1 mL·min^{-1}. A 2 μL aliquot of sample was directly injected with a split ratio of 1/30.

The initial oven temperature was set at 45 °C, followed by a linear increase rate of 5 °C·min^{-1} to 130 °C and a final linear increase rate of 15 °C·min^{-1} to 210 °C. The total running time per analysis was 22 min. The chromatographic data were acquired with the Hewlett-Packard Chemstation software B 0204 from Agilent Technologies.

The mass compositions of ethyl lactate were determined through calibration curves including butan-1-ol (CAS 71-36-3; mass purity, 99.50%; Carlo Erba. Val de Reuil, France) as internal standard to minimize variability. The calibration curves were established by diluting ethyl lactate in two different solvents: absolute ethanol and an ethanol−water mixture (ethanol mass fraction z_{mEt} = 0.5), in order to take account of the variations of injections and column performances due to matrix effects. In both calibration curves, the ethyl lactate mass fraction range varies from x_{mEL} = (0.2×10^{-4} to 50.0×10^{-4}), suitable for the analysis of the equilibrium samples. Seven calibration points were considered in both solvents.

The calculated detection and quantification limits derived from the analytical treatment of the calibration results were, respectively, DL = 6.5×10^{-6} g·g^{-1} and QL = 50.0×10^{-6} g·g^{-1} in absolute ethanol, and DL = 2.0×10^{-5} g·g^{-1} and QL = 14.0×10^{-5} g·g^{-1} in the ethanol−water mixture.

For mixtures with ethanol mass fractions lower than 0.50, a quantitative dilution in ethanol was done to reach z_{mEt} = 0.50 and the ethyl lactate compositions were calculated by using the calibration curve in the mixed solvent. For mixtures with higher ethanol fractions, the ethyl lactate compositions were calculated without any dilution. The calibration curve in absolute ethanol was used for mixtures with ethanol mass fractions between 0.75 and 1.00, and that in the mixed solvent, for mixtures with ethanol mass fractions between 0.50 and 0.75.

Each equilibrium sample as well as each calibration point was injected in triplicate. The relative standard uncertainty of the ratio between the ethyl lactate peak area and that of butan-1-ol, $u_r(R_{AEL\text{-}IS})$, varies from 0.05% to 5.03% with an average value of 0.44%. This result enables validation of the analysis repeatability, and therefore of the precision of the composition calculated with the calibration curves.

The initial ternary mixtures, before equilibrium, were also analyzed in order to validate the accuracy of the analysis. The relative deviation (AD%) between the mass fractions of ethyl lactate determined by weighing ($z_{mEL\text{-}EXP}$), and the analytical values estimated by gas chromatography ($z_{mEL\text{-}ANA}$) varies between 0.69% and 10.46%. Nonetheless, except for this upper limit, the deviations are inferior to 6.41% and the overall relative deviation (AAD %) is only around 4.62%. This value is quite acceptable in relation to the analysis technique and to the concentration level of ethyl lactate in the ternary solutions.

Ethanol Mass Fractions. The ethanol mass compositions in the liquid and vapor phases were computed from the following experimental data: temperature (T), pressure (P), and global initial composition of the mixed solvent (z_{Et}), by considering that the bubble temperature and compositions of ethanol and water depend exclusively on the ethanol−water binary equilibrium. This assumption is valid because the concentration of ethyl lactate in both phases is significantly low (maximum liquid mole fraction on the order of 10^{-4}), which means that its influence on the thermal and mechanical equilibriums of the system is negligible.[43]

The calculation was carried out using the Flash TP algorithm of the Simulis Thermodynamics Package by ProSim, which computes equilibrium compositions at fixed temperature, pressure, and global composition. The thermodynamic model used to represent the vapor−liquid equilibrium of the binary system ethanol−water at 101.3 kPa was NRTL, with the interaction parameters reported by Kadir.[50] The reliability of these parameters was verified by fitting the experimental data measured by different authors.[44,51−53] The average relative deviation between the experimental and the calculated temperatures was 0.2% and that of mole fractions in the vapor phase around 1.24%. The equilibrium diagram including the experimental data and the NRTL representation is presented in Figure 3.

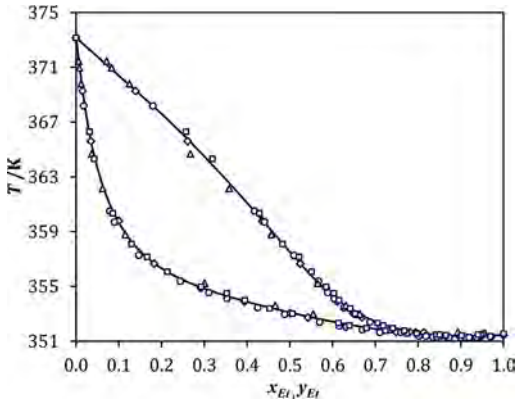

Figure 3. Equilibrium diagram of the binary system ethanol–water at 101.3 kPa: (◇) data by Lai et al, 2014;[44] (□) data by Arce et al, 1996;[51] (△) data by Yang and Wang, 2002;[52] (○) data by Kamihama et al, 2012;[53] (—) NRTL model using the interaction parameters calculated by Kadir.[50] T is the equilibrium temperature, x_{Et} the ethanol mole fraction in the liquid phase, and y_{Et} is the ethanol mole fraction in the vapor phase.

The calculation of ethanol mass fractions, instead of a measurement with a specific instrumental technique can be considered to be an acceptable approach for two reasons: (i) the experimental values of temperature and pressure are reliable enough and (ii) the NRTL model represents accurately the phase behavior of the mixed solvent. Moreover, it is important to point out that the real interest of our research is to represent the equilibrium distribution of ethyl lactate for simulation purposes, hence the *analytical effort* was focused on the quantification of this minor compound.

Mole Fractions. The mass fractions of water were calculated by difference. The mole fractions of the liquid and vapor phases were then computed from the mass fractions and the molar masses of the three compounds.

Computation of Uncertainties. The uncertainties of the equilibrium variables were calculated by using the law of propagation of uncertainties, as they were not measured directly but determined from other quantities through a functional relation.[54] The propagation of standard uncertainties is associated with four main factors: (1) the mass measurements with the weighing scales ($u(m_1) = 0.00006$ g for the first one and $u(m_2) = 0.006$ g for the second one), (2) the repeatability of the injections in chromatographic analysis, expressed in terms of the area ratio between the ethyl lactate and internal standard peaks ($0.001 \le u(R_{AEL\text{-}IS}) \le 0.081$), (3) the temperature measurements ($0.1\ \text{K} \le u(T) \le 0.3\ \text{K}$), and (4) the pressure measurements ($0.2\ \text{kPa} \le u(P) \le 0.5\ \text{kPa}$), both during the equilibrium experiments. The calculation was simplified by assuming that the estimates of the input quantities to calculate each equilibrium variable were uncorrelated. The computed values are presented in the results sections.

THERMODYNAMIC MODELING

In this section, some elements about the thermodynamic models used in this work are presented. A suitable choice of these models is fundamental in process simulation for a correct representation of the aroma compound behavior during distillation and other separation processes. For aroma compounds–ethanol–water systems at low pressures, the deviations from ideal behavior are usually associated with the liquid phase and can therefore be described with the excess Gibbs energy approach, widely used and recommended in the literature. Among the models of this approach, the semiempirical methods are considered in this work since they are easy for implementation and are available in most process simulators.

Fundamental Equation of Phase Equilibrium. Vapor–liquid phase equilibria are computed by satisfying the equality of fugacities of all components i present in the two phases:[55,56]

$$f_i^{V}(T, P, \mathbf{y}) = f_i^{L}(T, P, \mathbf{x}) \tag{1}$$

Here f_i^{V} and f_i^{L} are the vapor and liquid fugacity of the species i, respectively. This property is a function of the temperature (T), the pressure (P), and the corresponding vector of mole composition ($\mathbf{y}$ or $\mathbf{x}$).

Since the pressure is low (<1000 kPa) and always below the critical pressure of the pure components, the vapor phase can be assumed as an ideal gas mixture and the properties of the liquid phase are pressure independent. As a result, eq 1 can be approximated as

$$y_i P = \gamma_i(T, \mathbf{x}) x_i P_i^{o}(T) \tag{2}$$

In eq 2, γ_i is the activity coefficient of the species i in the liquid phase, $P_i^{o}(T)$ is the vapor pressure of pure compound, and y_i and x_i are the respective equilibrium mole fractions in the vapor and liquid phases.

The equilibrium behavior of an aroma compound (AC) in hydroalcoholic mixtures depends not only on the physical conditions (T, P) but also on the solvent composition (ethanol and water), and can be described by means of two properties: the partition coefficient and the relative volatility.

The partition coefficient (K_{AC}), also known as physical equilibrium constant or absolute volatility, represents the aroma compound distribution between the vapor and liquid phases and is defined as

$$K_{AC} = \frac{y_{AC}}{x_{AC}} \tag{3}$$

The relative volatility with respect to ethanol ($\alpha_{AC/Et}$), is an indicator of the species behavior during the distillation of aroma compounds–ethanol–water mixtures:[57]

$$\alpha_{AC/Et} = \frac{K_{AC}}{K_{Et}} = \frac{y_{AC}/x_{AC}}{y_{Et}/x_{Et}} = \frac{y_{mAC}/x_{mAC}}{y_{mEt}/x_{mEt}} \tag{4}$$

By combining eqs 2 and 3, the partition coefficient can also be computed as

$$K_i = \frac{y_i}{x_i} = \frac{\gamma_i(T, \mathbf{x}) P_i^{o}(T)}{P} \tag{5}$$

In the current study, it is useful to consider that ethyl lactate is placed in the region of infinite dilution, as this compound is present at very low concentrations (maximum liquid mole fraction on the order of 10^{-4}).

In this case, the Henry constant, $\mathcal{H}_i$ is defined by the following relation:[58]

$$\mathcal{H}_i(T, P, \mathbf{x}) = \lim_{x_i \to 0} \frac{f_i^{L}(T, P, \mathbf{x})}{x_i} \tag{6}$$

At low pressures, this variable can also be written as a function of $P_i^{o}(T)$ and $\gamma_i(T,x)$ at infinite dilution or $\gamma_i^{\infty}(T,\mathbf{x}_s)$, which depends on the temperature and solvent composition, $\mathbf{x}_s$:

Table 2. Coefficients of the Riedel Equation for Calculating Vapor Pressures in kPa at a Given Temperature in K[a]

component	A_i	B_i	C_i	D_i	E_i	T_{min}/K	T_{max}/K
ethyl lactate	78.774	−6715.3	−9.5666	1.4993×10^{-2}	1	247.2	588.0
ethanol	73.304	−7122.3	−7.1424	2.8853×10^{-6}	2	159.1	514.0
water	73.649	−7258.2	−7.3037	4.1653×10^{-6}	2	273.2	647.1

[a] T_{min} and T_{max} define the temperature interval of validity of the empirical equation. Information is available in Simulis thermodynamics package.

Table 3. Activity Coefficient (γ_i) Equations of NRTL and UNIQUAC Models[a]

reference	equations	parameters
	NRTL Model	
	$\ln \gamma_i(T, \mathbf{x}) = \frac{\sum_{j=1}^{n} \tau_{ji} G_{ji} x_j}{\sum_{k=1}^{n} G_{ki} x_k} + \sum_{j=1}^{n} \frac{G_{ij} x_j}{\sum_{k=1}^{n} G_{kj} x_k} \left(\tau_{ij} - \frac{\sum_{k=1}^{n} \tau_{kj} G_{kj} x_k}{\sum_{j=1}^{n} G_{kj} x_k} \right)$ (3.1)	
Renon and Prausnitz[63]	$G_{ij} = \exp(-c_{ij}\tau_{ij})$ (3.2)	•Binary interaction parameters A_{ij}^0, A_{ij}^T, c_{ij}^0, c_{ij}^T
	$c_{ij} = c_{ij}^0 + c_{ij}^T (T - 273.15)$ (3.3)	
	$\tau_{ij} = \frac{g_{ij} - g_{jj}}{RT} = \frac{A_{ij}^0 + A_{ij}^T (T - 273.15)}{RT}$ (3.4)	
	UNIQUAC Model	
	$ln\gamma_i(T, \mathbf{x}) = ln\gamma_i^C + ln\gamma_i^R$ (3.5)	
	combinatorial contribution, $\ln \gamma_i^C$	
	Staverman−Guggenheim term	
	$\ln\gamma_i^C = \ln\frac{\varphi_i}{x_i} + \frac{Z}{2} q_i \ln\frac{\theta_i}{\varphi_i} + l_i - \frac{\varphi_i}{x_i} \sum_{j=1}^{n} x_j l_j$ (3.6)	
	$l_i = \frac{Z}{2}(r_i - q_i) - (r_i - 1)$ (3.7)	•Coordination number, $Z = 10$
Abrams and Prausnitz[71]	$\varphi_i = \frac{r_i x_i}{\sum_{j=1}^{n} r_j x_j}$ (3.8)	•Van der Waals volume, r_i
Anderson and Prausnitz[72]	residual contribution, $\ln \gamma_i^R$	•Van der Waals surface, •q_i and q_i'
	$\ln \gamma_i^R = q'_i - q'_i \ln\left(\sum_{j=1}^{n} \theta_j \tau_{ji}\right) - q'_i \sum_{j=1}^{n} \frac{\theta'_i \tau_{ji}}{\sum_{k=1}^{n} \theta'_k \tau_{kj}}$ (3.9)	•Binary interaction parameters A_{ij}^0, A_{ij}^T
	$\theta_i = \frac{q_i x_i}{\sum_{j=1}^{n} q'_j x_j}$ (3.10)	
	$\theta'_i = \frac{q'_i x_i}{\sum_{j=1}^{n} q'_j x_j}$ (3.11)	
	$\tau_{ij} = \exp\left(-\frac{g_{ij} - g_{jj}}{RT}\right) = \exp\left(-\frac{A_{ij}^0 + A_{ij}^T T}{RT}\right)$ (3.12)	

[a] τ_{ij}, g_{ij}, G_{ij} are binary interaction variables between species i and j in both activities models. φ_i is a volume fraction, θ_i and θ'_i are surface fractions and l_i a supplementary parameter of the combinatorial contribution in the UNIQUAC model. R is the ideal gas constant (1.9872 cal·mol^{-1} ·K^{-1}) and n is the number of chemical species in the system, three in this work.

$$\mathcal{H}_i(T, \mathbf{x}_s) = \gamma_i^{\infty}(T, \mathbf{x}_s) P_i^{o}(T) \quad (7)$$

The activity coefficient at infinite dilution, γ_i^{∞}, provides accurate information about the aroma compound−mixed solvent interactions and therefore about the deviation from the ideal solution.[59]

In this work, the vapor pressure of the three compounds have been calculated with the Riedel equation,[60] an extended version of the Antoine equation:

$$P_i^{o}(T) = \frac{1}{1000} \exp\left(A_i + \frac{B_i}{T} + C_i \ln(T) + D_i T^{E_i}\right) \quad (8)$$

where $P_i^{o}(T)$ is given in kPa and T in K. A_i, B_i, C_i, D_i, and E_i are coefficients specific for each compound. They were taken from the DIPPR Database, available through the Simulis Thermodynamics Package, and are summarized in Table 2. According to the values of T_{min} and T_{max}, the coefficients are valid for the three compounds in the temperature range of the equilibrium measurements (from 352.3 to 370.0) K.

Calculation of Activity Coefficients. With regard to the activity coefficient, two semiempirical models of the excess Gibbs energy (G^E) approach were used in this work: NRTL and UNIQUAC. Both models provide pressure-independent activity coefficients as a function of temperature and composition.[61] The main working equations are presented in this section. The reader is directed to the principal references indicated for each model for further details about their theoretical basis.

The non-random two liquid (NRTL) and universal quasichemical (UNIQUAC) models of liquid solution are based on the concept of local composition as introduced by

Wilson.[62] They are valid at low pressures (<1000 kPa) and are widely recommended for the description of hydroalcoholic solutions. The activity coefficient of a component i as a function of composition and temperature is given by the equations summarized in Table 3. The UNIQUAC pure compound parameters for the three species studied in this work are presented in Table 4.

Table 4. UNIQUAC Parameters for the Studied System

component	r_i[a]	q_i[a]	q_i'[b]
ethyl lactate	4.4555	3.9280	3.9280
ethanol	2.1055	1.9720	0.9600
water	0.9200	1.4000	1.0000

[a]Delgado et al.[37] [b]Anderson and Prausnitz.[72] r_i is the van der Waals volume, and q_i and q_i' are the van der Waals surfaces.

In both semiempirical models, the temperature dependence of c_{ij} and τ_{ij} is evaluated according to the original formalisms, included in the Simulis Thermodynamics package. The variables A_{ij}^0, A_{ij}^T (non-symmetric), c_{ij}^0 and c_{ij}^T (symmetric) are binary interaction parameters specific to each system. They must be obtained by regression of experimental equilibrium data and/or other thermophysical properties of the liquid phase. The estimation of these parameters for the studied system is presented in the results section.

RESULTS AND DISCUSSION

Experimental Data. The vapor−liquid equilibrium data of the ternary system at 101.3 kPa are given in Table 5. To characterize the behavior of ethyl lactate in the hydroalcoholic medium, the values of γ_{EL}^{∞}, $\mathcal{H}_{EL}$, K_{EL}, and $\alpha_{EL/Et}$ are reported in Table 6. Activity coefficients and Henry constants derive from the equilibrium relations, eq 2 and eq 7, and volatilities were directly calculated from composition data, according to eq 3 and eq 4. For the measurements of temperature and pressure, the values are reported with their respective standard uncertainties. For the other equilibrium variables, the reported uncertainties are the combined expanded ones, using a confidence level of 95% that corresponds to a coverage factor of $k = 2$.

The evolution of absolute and relative volatilities as a function of ethanol composition in the liquid phase is presented in Figure 4. According to this figure, the volatility of ethyl lactate decreases with the increasing ethanol concentration in the liquid phase.

Table 5. Vapor-Liquid Equilibrium Data of the System Ethyl Lactate Highly Diluted (EL)−Ethanol (Et)−Water (W) at P = 101.3 kPa[a]

			mole composition of liquid phase (x)						mole composition of vapor phase (y)					
T/K	$u(T)$ /K	$u(P)$ /kPa	x_{EL}	$U_c(x_{EL})$	x_{Et}	$U_c(x_{Et})$	x_W	$U_c(x_W)$	y_{EL}	$U_c(y_{EL})$	y_{Et}	$U_c(y_{Et})$	y_W	$U_c(y_W)$
exp	calc	calc	exp	calc	calc	calc	calc	calc	exp	calc	calc	calc	calc	calc
370.0	0.3	0.2	1.38×10^{-4}	1.08×10^{-6}	0.012	3.35×10^{-4}	0.988	3.35×10^{-4}	3.81×10^{-4}	7.85×10^{-6}	0.117	3.40×10^{-3}	0.882	3.40×10^{-3}
365.6	0.1	0.2	1.62×10^{-4}	8.29×10^{-7}	0.035	6.40×10^{-4}	0.965	6.40×10^{-4}	3.02×10^{-4}	2.10×10^{-6}	0.264	4.84×10^{-3}	0.735	4.84×10^{-3}
363.8	0.1	0.2	1.64×10^{-4}	1.26×10^{-6}	0.049	9.03×10^{-4}	0.951	9.03×10^{-4}	2.44×10^{-4}	5.89×10^{-6}	0.321	5.91×10^{-3}	0.678	5.91×10^{-3}
363.7	0.1	0.2	1.55×10^{-4}	1.36×10^{-6}	0.050	9.59×10^{-4}	0.950	9.59×10^{-4}	2.31×10^{-4}	5.48×10^{-6}	0.323	6.26×10^{-3}	0.677	6.26×10^{-3}
362.0	0.1	0.2	1.82×10^{-4}	1.24×10^{-6}	0.066	1.23×10^{-3}	0.934	1.23×10^{-3}	2.37×10^{-4}	2.07×10^{-6}	0.375	6.92×10^{-3}	0.624	6.92×10^{-3}
362.0	0.2	0.3	1.77×10^{-4}	6.38×10^{-6}	0.066	1.69×10^{-3}	0.934	1.69×10^{-3}	2.34×10^{-4}	3.31×10^{-6}	0.376	9.50×10^{-3}	0.623	9.50×10^{-3}
360.0	0.1	0.2	1.78×10^{-4}	8.96×10^{-7}	0.095	1.76×10^{-3}	0.905	1.76×10^{-3}	1.30×10^{-4}	1.14×10^{-6}	0.432	8.00×10^{-3}	0.567	8.00×10^{-3}
359.1	0.1	0.5	1.83×10^{-4}	9.44×10^{-7}	0.111	2.06×10^{-3}	0.889	2.06×10^{-3}	1.16×10^{-4}	1.70×10^{-6}	0.457	8.47×10^{-3}	0.543	8.47×10^{-3}
358.9	0.1	0.4	1.76×10^{-4}	3.03×10^{-6}	0.114	2.12×10^{-3}	0.886	2.12×10^{-3}	1.21×10^{-4}	1.20×10^{-6}	0.461	8.55×10^{-3}	0.539	8.55×10^{-3}
358.3	0.1	0.3	1.92×10^{-4}	1.07×10^{-6}	0.129	2.40×10^{-3}	0.871	2.40×10^{-3}	7.23×10^{-5}	7.33×10^{-7}	0.479	8.89×10^{-3}	0.521	8.89×10^{-3}
358.2	0.1	0.5	1.80×10^{-4}	9.48×10^{-7}	0.130	2.44×10^{-3}	0.869	2.44×10^{-3}	7.72×10^{-5}	1.04×10^{-6}	0.481	8.93×10^{-3}	0.519	8.93×10^{-3}
357.8	0.1	0.4	2.17×10^{-4}	2.84×10^{-6}	0.143	2.66×10^{-3}	0.857	2.66×10^{-3}	8.56×10^{-5}	1.01×10^{-6}	0.494	9.17×10^{-3}	0.506	9.17×10^{-3}
357.7	0.1	0.4	2.02×10^{-4}	2.18×10^{-6}	0.146	2.72×10^{-3}	0.854	2.72×10^{-3}	8.28×10^{-5}	1.65×10^{-6}	0.496	9.22×10^{-3}	0.503	9.22×10^{-3}
353.9	0.1	0.5	2.68×10^{-4}	2.70×10^{-5}	0.392	7.35×10^{-3}	0.608	7.35×10^{-3}	2.89×10^{-5}	1.32×10^{-6}	0.615	1.15×10^{-2}	0.385	1.15×10^{-2}
353.9	0.1	0.3	2.71×10^{-4}	6.06×10^{-6}	0.401	7.52×10^{-3}	0.599	7.52×10^{-3}	3.21×10^{-5}	1.11×10^{-6}	0.618	1.16×10^{-2}	0.382	1.16×10^{-2}
352.3	0.1	0.5	3.45×10^{-4}	3.76×10^{-6}	0.624	1.18×10^{-2}	0.375	1.18×10^{-2}	2.75×10^{-5}	3.81×10^{-7}	0.714	1.35×10^{-2}	0.286	1.35×10^{-2}
352.3	0.1	0.4	2.82×10^{-4}	3.10×10^{-6}	0.626	1.18×10^{-2}	0.374	1.18×10^{-2}	2.38×10^{-5}	6.96×10^{-7}	0.715	1.35×10^{-2}	0.285	1.35×10^{-2}

[a]T and the equilibrium temperature of the vapor and liquid phases; u is the standard uncertainty, and U_c is the expanded combined uncertainty (95% level of confidence, $k = 2$). Notation: exp, experimental value (directly or indirectly measured with in an instrument); calc, calculated value (analytical estimation from experimental values).

Table 6. Equilibrium Variables Describing the Behavior of Ethyl Lactate Highly Diluted in Hydro-alcoholic Mixtures at P = 101.3 kPa[a]

		activity coefficients		Henry constants		absolute volatility		relative volatility	
T/K	x_{Et}	γ_{EL}^{∞}	$U_c(\gamma_{EL}^{\infty})$	$\mathcal{H}_{EL}$/kPa	$U_c(\mathcal{H}_{EL})$/kPa	K_{EL}	$U_c(K_{EL})$	$\alpha_{EL/Et}$	$U_c(\alpha_{EL/Et})$
exp	calc	calc	calc	calc	calc	calc	calc	calc	calc
370.0	0.012	18.89	0.66	278.97	12.31	2.75	6.07×10^{-2}	0.27	1.18×10^{-2}
365.6	0.035	15.19	0.22	189.50	3.54	1.87	1.61×10^{-2}	0.25	5.61×10^{-3}
363.8	0.049	12.98	0.37	150.18	4.59	1.49	3.78×10^{-2}	0.23	7.37×10^{-3}
363.7	0.050	13.03	0.37	151.05	4.77	1.48	3.75×10^{-2}	0.23	7.49×10^{-3}
362.0	0.066	12.41	0.20	133.88	2.68	1.30	1.44×10^{-2}	0.23	5.08×10^{-3}
362.0	0.066	12.21	0.55	131.88	6.66	1.32	5.12×10^{-2}	0.23	1.09×10^{-2}
360.0	0.095	7.42	0.12	73.91	1.47	0.73	7.35×10^{-3}	0.16	3.29×10^{-3}
359.1	0.111	7.31	0.13	69.89	1.53	0.63	9.85×10^{-3}	0.15	3.58×10^{-3}
358.9	0.114	6.68	0.17	64.14	1.81	0.69	1.37×10^{-2}	0.17	4.48×10^{-3}
358.3	0.129	4.10	0.07	38.19	0.79	0.38	4.36×10^{-3}	0.10	2.06×10^{-3}
358.2	0.130	4.67	0.09	43.33	0.98	0.43	6.17×10^{-3}	0.12	2.56×10^{-3}
357.8	0.143	4.58	0.09	41.59	1.00	0.39	6.94×10^{-3}	0.11	2.73×10^{-3}
357.7	0.146	4.38	0.12	39.91	1.18	0.41	9.32×10^{-3}	0.12	3.36×10^{-3}
353.9	0.392	1.55	0.15	12.01	1.16	0.11	1.14×10^{-2}	0.07	7.24×10^{-3}
353.9	0.401	1.40	0.07	10.93	0.53	0.12	4.88×10^{-3}	0.08	3.24×10^{-3}
352.3	0.624	1.11	0.02	8.08	0.20	0.08	1.41×10^{-3}	0.07	1.20×10^{-3}
352.3	0.626	1.18	0.04	8.54	0.31	0.08	2.64×10^{-3}	0.07	2.29×10^{-3}

[a] T is the equilibrium temperature of the vapor and liquid phases. x_{Et} is the mole fraction of ethanol in the liquid phase at equilibrium. U_c is the combined expanded uncertainty (95% level of confidence, k = 2). Notation: exp, experimental value (directly or indirectly measured with in an instrument); calc, calculated value (analytical estimation from experimental values).

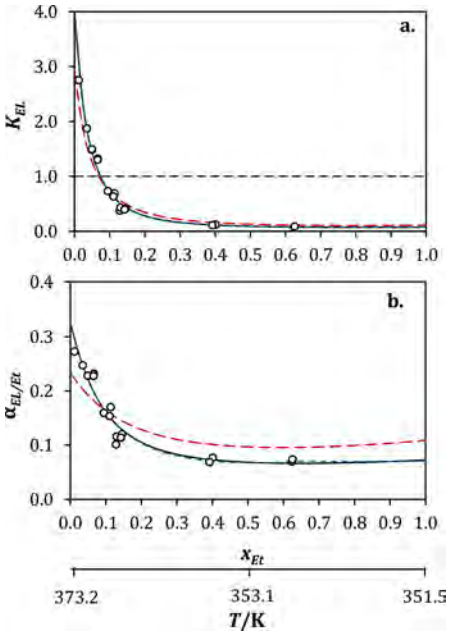

Figure 4. Evolution of (a) absolute (K_{EL}) and (b) relative volatilities ($\alpha_{EL/Et}$) of ethyl lactate at 101.3 kPa as a function of ethanol composition (x_{Et} mole fraction) in the liquid phase: (○) experimental data, (black solid line) NRTL model, (blue short dash) UNIQUAC model, (red long dash) UNIQUAC model with literature interaction parameters, fitted to binary data.[35,37] T is the corresponding equilibrium temperature.

This behavior, already identified for other aroma compounds highly diluted,[42,43] can be explained by two reasons: (1) the equilibrium temperature of the system decreases as the ethanol liquid concentration is increased (according to the *Txy* diagram, Figure 3) which leads to a reduction of the vapor pressure of the aroma compound and (2) the chemical nature of the aroma compound is closer to ethanol (presence of a carbon chain and of a C−OH (carbon−hydroxyl) bond) than to water. Thus, when the system is enriched with the organic solvent (ethanol), the difference between the cohesive forces (like molecules) and adhesive forces (unlike molecules) in the liquid phase is reduced and the transition of ethyl lactate to the vapor phase becomes less favorable.

According to Figure 4a, the vapor phase is richer in ethyl lactate (K_{EL} > 1) when the liquid ethanol mole fraction is lower than x_{Et} = 0.1. For higher fractions, the phenomenon is reversed and the aroma compound becomes 2 to 10 times more abundant in the liquid phase. Concerning the relative volatility, ethanol is more volatile than ethyl lactate over the entire concentration range of the solvent, as evidenced in Figure 4b. This volatility ratio varies by a factor of 4, from 0.27, when x_{Et} tends to 0, to 0.07, when x_{Et} tends to 1.

Modeling with Semiempirical Models. Experimental equilibrium data were correlated by using the NRTL and UNIQUAC models. The objective was to determine the interaction parameters for the binary subsystems: ethyl lactate (1)−ethanol (2), ethyl lactate (1)−water (3) and ethanol (2)−water (3), which corresponds to 18 parameters for the NRTL model and 12 for the UNIQUAC model.

To reduce the number of parameters, the following assumptions were considered:

- For the NRTL model, the non-randomness parameter, c_{ij}^{0}, was set to 0.3 for all binaries. This assumption is valid for systems in vapor−liquid equilibrium containing water and polar non-associated substances.[63]
- For the ethyl lactate−ethanol and ethyl lactate−water binaries, A_{ij}^{T}, the temperature-dependent parameters of τ_{ij}, were neglected. Two factors justify this approximation: (1) the number of experimental data is limited and (2) the equilibrium temperature interval is reduced (from 352.3 to 370.0) K.

Table 7. Interaction Parameters for the Binary Ethanol (2) − Water (3) and Fitting Quality Statistics with Respect to Five Experimental Data Sets Obtained from Literature[a]

					T/K		y_{Et}	
model	A^0_{23}/cal·mol^{-1}	A^0_{32}/cal·mol^{-1}	A^0_{23}/cal·mol^{-1}·K^{-1}	A^T_{32}/cal·mol^{-1}·K^{-1}	AAD%	RMSE	AAD%	RMSE
NRTL[b]	34.02	850.12	−1.8	5.65	0.2	0.3	1.24	0.01
UNIQUAC[c]	1448.61	−1504.21	−3.68	4.96	0.2	0.3	1.27	0.01

[a]These parameters are fixed for the correlation of equilibrium data of the ternary system ethyl lactate highly diluted—ethanol—water. [b]Kadir.[50] [c]Delgado et al.[37] Notation: T, equilibrium temperature; y_{Et}, ethanol mole fraction in the vapor phase; AAD%, average absolute deviation; RMSE, root-mean-squared deviation.

- The interaction parameters of the binary ethanol (2)−water (3) are fixed to the values presented in the literature[50] and reported in Table 7. In this case, the temperature dependency is considered ($A^T_{ij} \neq 0$) as this major binary governs the thermal equilibrium of the ternary system. As previously stated, the reliability of the interaction parameters was verified by fitting different experimental data sets.[44,51−53] The deviations of the temperature and vapor mole fractions calculated with NRTL and UNIQUAC models are also reported in Table 7. According to this information, the experimental data from the literature are well correlated by both models, with average relative deviations of 0.2% for temperature and lower than 1.3% for ethanol mole fractions in the vapor phase. A detailed procedure to assess the thermodynamic consistency of the reference data is presented in Appendix 1.

In this way, the model identification for the ternary system is reduced to the regression of four parameters:

- two associated with the binary ethyl lactate (1)−ethanol (2): A^0_{12}, A^0_{21}.
- two associated with the binary ethyl lactate (1)−water (3): A^0_{13}, A^0_{31}.

The parameters were fitted by minimizing an objective function with the generalized reduced gradient method.[64] The regressed properties were K_{EL} and $\alpha_{EL/Et}$. These parameters will be considered for the simulation of distillation units, in which the separation performance is directly based upon the difference of volatilities between the chemical species.

Two objective functions were evaluated:

$$\mathrm{OF}(\alpha) = \sum_{i=1}^{N} w_i(\alpha_{\mathrm{EL/Et}\,i\,\mathrm{Exp}} - \alpha_{\mathrm{EL/Et}\,i\,\mathrm{Model}})^2 \tag{9}$$

$$\mathrm{OF}(K) = \sum_{i=1}^{N} w_i(K_{\mathrm{EL}\,i\,\mathrm{Exp}} - K_{\mathrm{EL}\,i\,\mathrm{Model}})^2 \tag{10}$$

where N is the number of data and w_i is a weighting factor depending on the uncertainty of the experimental data ($\alpha_{\mathrm{EL/Et}\ i\ \mathrm{Exp}}$, $K_{\mathrm{EL}\ i\ \mathrm{Exp}}$). An experimental value having a high standard uncertainty is supposed to be less reliable and has therefore a lower weighting factor than an experimental value with a low uncertainty.

The weighting factors were normalized ($\sum w_i = 1$) and calculated as

$$w_i = \frac{1/U_c(i)}{\sum_{i=1}^{N} 1/U_c(i)} \tag{11}$$

where U_c is the estimated expanded combined uncertainty for each experimental value.

The calculation of equilibrium properties ($\alpha_{\mathrm{EL/Et}\,i\,\mathrm{Model}}$, $K_{\mathrm{EL}\ i\ \mathrm{Model}}$) was carried out using the bubble temperature algorithm of the Simulis Thermodynamics package, at the experimental pressure (P) and composition in the liquid phase (x). The algorithms allow computation of the saturated temperature (T), and the composition of the vapor phase (y) in equilibrium.

The fitting quality was judged with respect to four variables (E): T, y_{Et}, and y_{EL}, K_{EL}, and $\alpha_{EL/Et}$. Two deviations were calculated:

- Average absolute relative deviation (AAD%):

$$\mathrm{AAD\%} = \frac{1}{N}\sum_{i=1}^{N}\left|\frac{E_{i\mathrm{Exp}} - E_{i\mathrm{Model}}}{E_{i\mathrm{Exp}}}\right| 100 \tag{12}$$

- Root-mean-squared deviation (RMSE):

$$\mathrm{RMSE} = \left[\frac{1}{N}\sum_{i=1}^{N}(E_{i\mathrm{Exp}} - E_{i\mathrm{Model}})^2\right]^{1/2} \tag{13}$$

The results obtained are summarized in Table 8. The evaluation of the thermodynamic consistency of the experimental data set reported in this work is complicated as one of the species is present at very low concentrations. No specific consistency tests have been reported in the literature for this type of system. The area test proposed by Kurihara et al.[65] cannot be used as the ethyl lactate does not cover the entire composition range. Therefore, only the point-to-point test, developed by Van Ness et al.[66] was considered for validation. This test should be regarded as a modeling capability test, which shows how the NRTL and UNIQUAC model can accurately reproduce the experimental data. After completion of the model identification, the approved criteria applied in this work are the AAD% values of y_{EL}, K_{EL}, and $\alpha_{EL/Et}$. To pass the test the values of those criteria must be less than a selected tolerance, fixed at 10% by Faundez et al.[67] As a result, comparing the statistics reported in Table 8, one can conclude that for both models, only the regressions based on OF($\alpha_{EL/Et}$) are consistent.

To complete the consistency test, the absolute (Δ) and relative (AD%) residuals of the equilibrium variables are plotted in Figure 5 as a function of the ethanol mole fraction x_{Et}. As suggested by Van Ness et al.[66] the data set passes the test if the residuals show a rather random distribution about the zero line with low deviations. In this case, even though it is difficult to define whether the scatter distribution is actually random due to a limited number of points, the point-to-point consistency of the experimental data can be validated as the residuals do not follow any tendency or correlation with the liquid phase composition. The residual values are not negligible but they remain acceptable if one considers the difficulty to quantify with high accuracy the composition of ethyl lactate highly diluted.

Table 8. Binary Interaction Parameters for the Ternary System Ethyl Lactate Highly Diluted (1)−Ethanol (2)−Water (3) and Fitting Quality Statistics[a]

OF	binary i–j	A_{ij}^0/cal·mol^{-1}	A_{ji}^0/cal·mol^{-1}	T/K		y_{Et}		y_{EL}		K_{EL}		$\alpha_{EL/Et}$	
				AAD%	RMSE	AAD%	RMSE	AAD%	RMSE	AAD%	RMSE	AAD%	RMSE
						NRTL Model							
$\alpha_{EL/Et}$	(1)−(2)	455.52	−343.55	0.0	0.1	0.34	1.94×10^{-3}	9.63	1.70×10^{-5}	9.63	1.00×10^{-1}	9.59	1.79×10^{-2}
	(1)−(3)	−349.32	2758.14										
K_{EL}	(1)−(2)	54.97	−639.44	0.0	0.1	0.34	1.94×10^{-3}	15.51	1.57×10^{-5}	15.51	8.43×10^{-2}	15.49	2.10×10^{-2}
	(1)−(3)	386.75	1969.48										
						UNIQUAC Model							
$\alpha_{EL/Et}$	(1)−(2)	458.20	−213.76	0.0	0.1	0.43	1.72×10^{-3}	9.09	1.76×10^{-5}	9.09	1.08×10^{-2}	8.98	1.76×10^{-2}
	(1)−(3)	−184.94	575.61										
K_{EL}	(1)−(2)	448.13	−363.72	0.0	0.1	0.44	1.73×10^{-3}	14.34	1.61×10^{-5}	14.34	8.77×10^{-2}	14.37	2.07×10^{-2}
	(1)−(3)	276.67	117.55										

[a]OF is the objective function used to determine the interaction parameters, T is the equilibrium temperature, y_{Et} is the ethanol mole fraction in the vapor phase, y_{EL} is the ethyl lactate mole fraction in the vapor phase, K_{EL} is the ethyl lactate absolute volatility, $\alpha_{EL/Et}$ is the ethyl lactate relative volatility with respect to ethanol, AAD% is the average absolute deviation, and RMSE is the root-mean-squared deviation.

In this way, using the interaction parameters derived from OF($\alpha_{EL/Et}$), the obtained evolution of K_{EL} and $\alpha_{EL/Et}$ as a function of ethanol composition is shown in Figure 4. Both models correlate correctly the experimental data. A very slight difference is noted only at high ethanol concentrations, from x_{Et} = 0.6.

Comparison with Literature Data. Concerning the information from the literature, the interaction parameters for ethyl lactate−ethanol and ethyl lactate−water pairs have been reported for the UNIQUAC model by Peña-Tejedor et al[35] and Delgado et al.[37] The values are presented in Table 9. They were estimated from isobaric experimental data of the corresponding binary systems, in which ethyl lactate is present over the entire composition range, from x_{EL}= (0 to 1).

The volatility curves of ethyl lactate as a function of ethanol composition, calculated with these latter parameters, are shown in Figure 4. The values of RMSE and AAD% for the different equilibrium values are summarized in Table 9. One can observe that the representation of the experimental data for the ternary system is globally acceptable, but the evolution of $\alpha_{EL/Et}$ with respect to ethanol composition exhibits some non-negligible differences: the volatility is underestimated at low ethanol concentrations ($x_{Et} \leq 0.1$), with an average error of 16%, and overestimated from x_{Et} = 0.1, with a mean error of about 29%. As a result, for simulation purposes in alcoholic beverages distillation, where relative volatility is the key parameter of separation, the interaction parameters proposed in this work (Table 8) are recommended.

Evolution of γ_{EL}^{∞} and $\mathcal{H}_{EL}$ with Temperature and Ethanol Composition. The evolution of the activity coefficient of ethyl lactate, γ_{EL}^{∞}, as a function of temperature and ethanol composition is shown in Figure 6. The activity coefficient is always higher than unity. In this case, the positive deviation from ideality ($\gamma_{EL}^{\infty} > 1$) means that the interactions forces between the solvent molecules and the ethyl lactate molecules are unfavorable, especially with water. It is observed that γ_{EL}^{∞} increases as the equilibrium temperature is increased and decreases when the liquid phase is enriched in ethanol. Both trends are linked since the activity coefficient is determined along the ethanol−water vapor−liquid equilibrium curve. The increase of γ_{EL}^{∞} indicates that the interaction forces between the ethyl lactate molecules are reduced, which leads to an increase of its partial pressure and therefore of its volatility. This behavior is logical since the volatility of ethyl lactate is higher in the low ethanol concentration region, where equilibrium temperatures are higher.

Concerning the Henry constant, the evolution of ln $\mathcal{H}_{EL}$ as a function of $1/T$ (plotted in Figure 7), calculated with the NRTL and UNIQUAC models, exhibits not a linear trend but a concave decreasing behavior. This can be explained by the fact that the temperature and the composition of the liquid phase are not independent at boiling conditions: a change in boiling temperature corresponds to a variation in the liquid composition and vice versa. As noted in eq 7, $\mathcal{H}_{EL}$ is a function of both temperature and composition, as the solvent is not a pure compound but a mixture of ethanol and water.

CONCLUSIONS

The vapor−liquid equilibrium of ethyl lactate highly diluted in ethanol−water mixtures at 101.3 kPa for boiling temperatures from (352.3 to 370.0) K was investigated in this work. The experimental results showed that the volatility of ethyl lactate

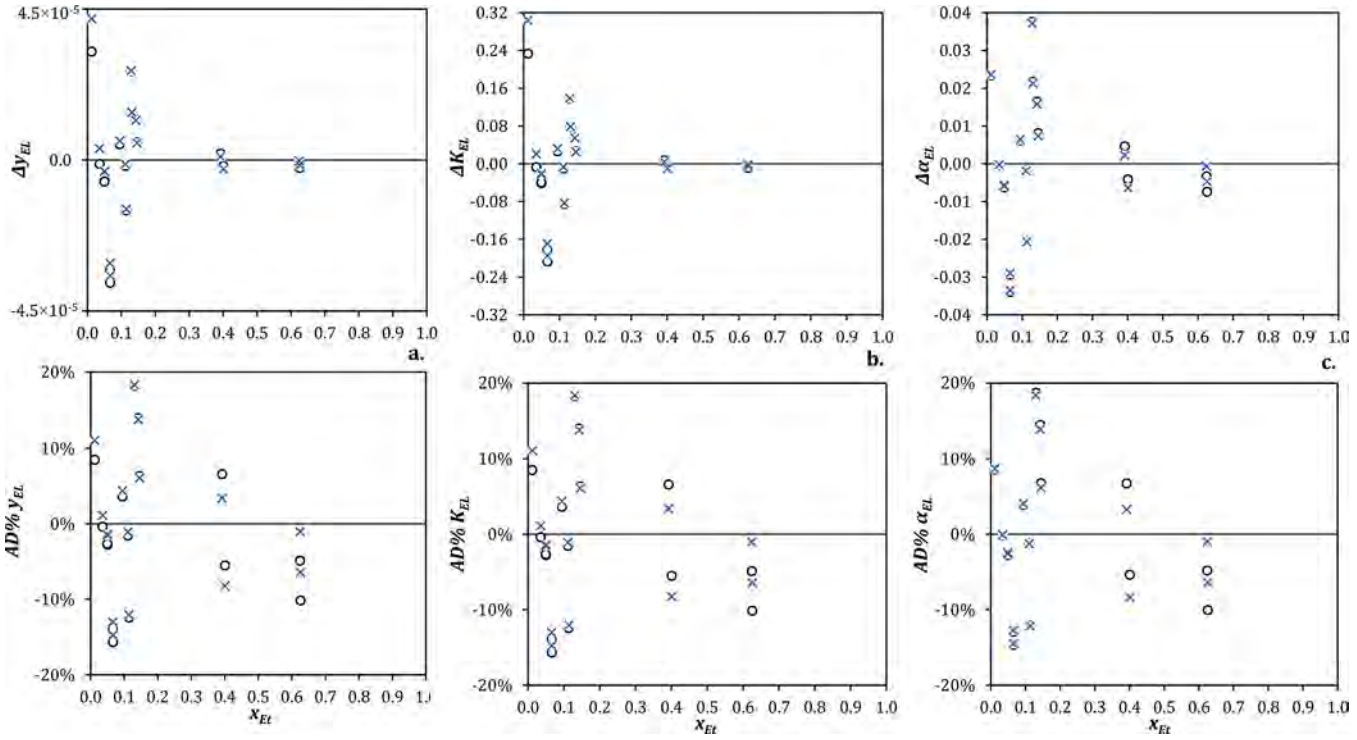

Figure 5. Plot of absolute (Δ) and relative (AD%) residuals of (a) y_{EL} (ethyl lactate mole fraction in the vapor phase), (b) K_{EL} (ethyl lactate absolute volatility) and (c) $\alpha_{EL/Et}$ (ethyl lactate relative volatility with respect to ethanol) at 101.3 kPa as a function of ethanol composition (x_{Et} mole fraction) in the liquid phase: (○) residuals for the NRTL model, (×) residuals for the UNIQUAC model.

Table 9. Interaction Parameters of UNIQUAC Models for the Binaries Ethyl Lactate (1)−Ethanol (2) and Ethyl Lactate (1)−Water (3) from the Literature. Fitting Quality Statistics of the Equilibrium Data Measured in This Work[a]

			T/K		y_{Et}		y_{EL}		K_{EL}		$\alpha_{EL/Et}$	
binary $i-j$	A_{ij}^0/cal·mol^{-1}	A_{ji}^0/cal·mol^{-1}	AAD%	RMSE	AAD%	RMSE	AAD%	RMSE	AAD%	RMSE	AAD%	RMSE
(1)−(2)[b]	679.2	−295.4	0.1	0.1	0.44	$1.77E \times 10^{-3}$	23.11	3.15×10^{-5}	23.11	1.92×10^{-1}	23.34	3.41×10^{-2}
(1)−(3)[c]	198.3	128.2										

[a] T is the equilibrium temperature, y_{Et} is the ethanol mole fraction in the vapor phase, y_{EL} is the ethyl lactate mole fraction in the vapor phase, K_{EL} is the ethyl lactate absolute volatility, $\alpha_{EL/Et}$ is the ethyl lactate relative volatility with respect to ethanol, AAD% is the average absolute deviation, and RMSE is the root-mean-squared deviation. [b] Peña-Tejedor et al.[35] [c] Delgado et al.[37]

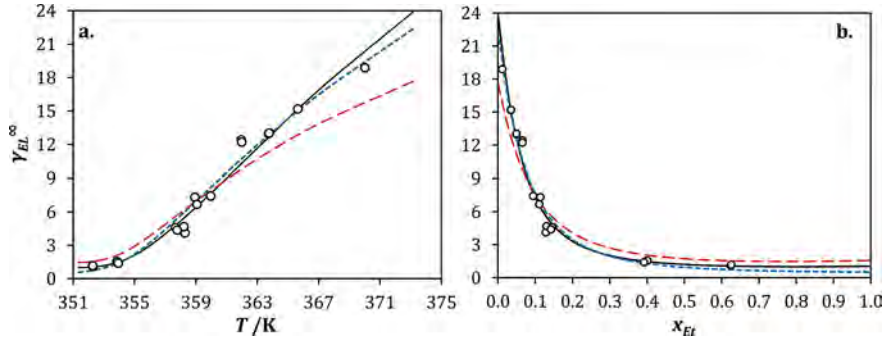

Figure 6. Evolution of the activity coefficient of ethyl lactate (γ_{EL}^{∞}) with respect to (a) equilibrium temperature (T) at 101.3 kPa and (b) ethanol composition in the liquid phase (x_{Et}): (○) experimental data, (black solid line) NRTL model, (blue short dash) UNIQUAC model, (red long dash) UNIQUAC with interaction parameters fitted to binary data.[35,37]

decreases when the ethanol content in the liquid phase is increased. Ethyl lactate is less volatile than ethanol and its relative volatility is reduced by a factor of four over the entire solvent composition range in the liquid phase. The ternary system exhibits positive deviation from ideality ($\gamma_i > 1$).

Good agreement between the measured data and the NRTL and UNIQUAC models was verified, with overall average relative deviations between 0.3% and 9.63%. The parameters calculated in this work can be used for simulation purposes in alcoholic beverages distillation, where ethyl lactate is present at low concentrations. Furthermore, the methodology of data acquisition and model identification here proposed can be used when dealing with other volatile aroma compounds in hydroalcoholic mixtures.

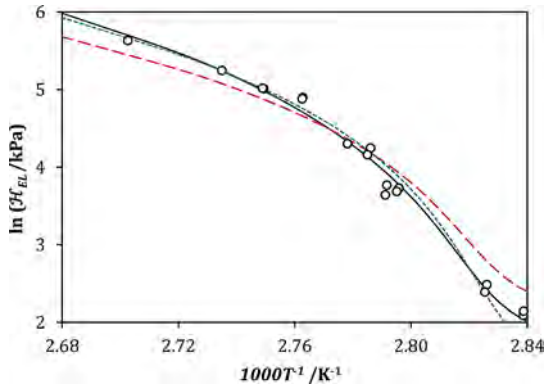

Figure 7. Representation of Ln $\mathcal{H}_{EL}$ with respect to $1/T$ at 101.3 kPa: (○) experimental data, (black solid line) NRTL model, (blue short dash) UNIQUAC model, (red short dash) UNIQUAC model with interaction parameters fitted to binary data.[35,37] $\mathcal{H}_{EL}$ is the Henry constant of ethyl lactate and T is the equilibrium temperature.

APPENDIX 1

Test of Thermodynamic Consistency for Experimental Vapor−liquid Data of Binary Ethanol−water at 101.3 kPa

The thermodynamic consistency of the experimental data used as reference to validate the interaction parameters for the binary ethanol−water was assessed by means of two tests: area test by Kurihara et al.[65] and point-to-point test proposed by Van Ness et al.[66] The aim of these tests is to validate the quality of experimental data and to perform preliminary data reduction.

Area Test. The area test is derived from the integration of the Gibbs−Duhem relation.[68] At isobaric conditions, the following expression is used:

$$A^* = 100 \times \left| \int_0^1 \ln \frac{\gamma_{Et}}{\gamma_W} \, dx_{Et} + \int_0^1 \varepsilon \, dx_{Et} \right| \quad (A1)$$

ε is a function of the excess enthalpy (H^E) and temperature:

$$\varepsilon = -\frac{H^E}{RT^2}\frac{\partial T}{\partial x_{Et}} \quad (A2)$$

The experimental data pass the area test if the value of A^* is lower than 3.[65] In this work, the arguments of the integral were calculated as follows:

- The activity coefficients γ_{Et} and γ_W were directly obtained from equilibrium data by using the fundamental equilibrium relation, eq 2:

$$\gamma_i = \frac{y_i P}{x_i P_i^o(T)} \quad (A3)$$

  The vapor pressures were computed with eq 8, using the coefficients gathered in Table 2.
- The excess enthalpy were estimated by means of the empirical correlation proposed by Larkin,[69] based on the adjustment of several experimental data sets:

$$H^E = x_{Et}(1 - x_{Et}) \sum_{i=0}^{m} a_i x_{Et}^{\ i} \quad (A4)$$

  Where H^E is given in J·mol^{-1}, i is a non-integral counter ($i = 0, 0.5, 1.5, 2.5, 4.5$) and a_i are temperature-dependent coefficients, computed as follows:

$$a_i = b_i + c_i T + d_i T^2 \quad (A5)$$

  The values of b_i, c_i, and d_i are reported by Larkin.[69]
- The relation between T and x_{Et} was evaluated by adjusting the experimental equilibrium data to a polynomial-type correlation with order 6, in the form of eq A6 ($n = 6$), with a coefficient of determination (R^2) higher than 0.99. F_i are coefficients determined from regression, by minimizing

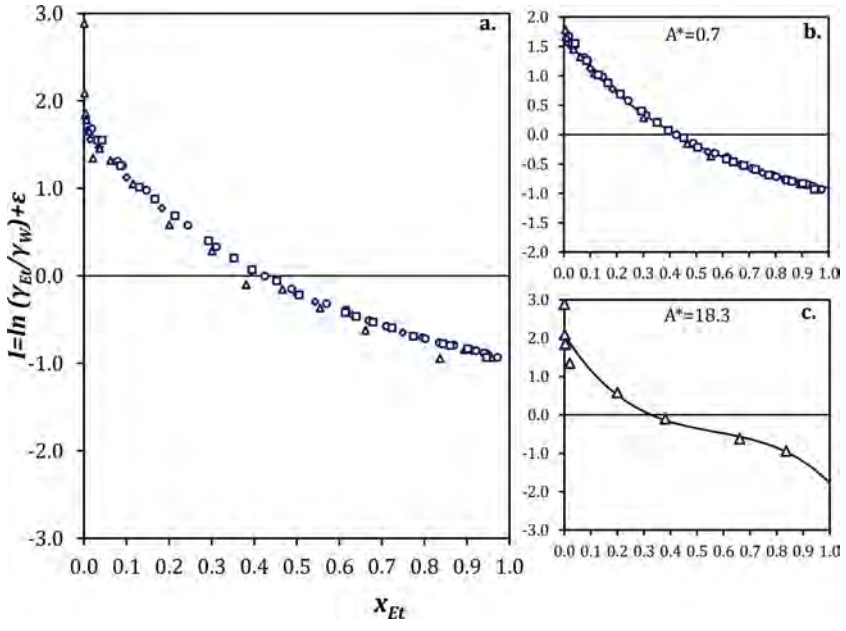

Figure A1. Plot of the area test for the reference equilibrium data of binary ethanol−water: (a) representation with all the experimental points, without data rejection; (b) representation after data rejection; (c) representation of rejected data, with appreciable deviation from global trend. (◇) Data by Lai et al, 2014.[44] (□) data by Arce et al, 1996.[51] (△) data by Yang and Wang, 2002.[52] (○) data by Kamihama et al, 2012;[53] (—) smoothing of the experimental data with a polynomial correlation.

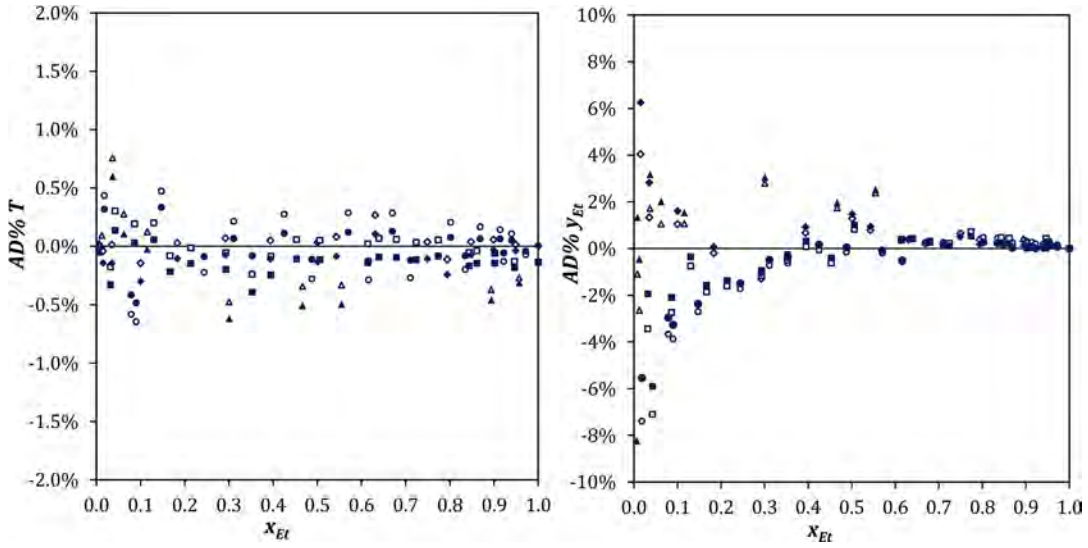

Figure A2. Plot of relative residual (AD%) for T and y_{Et} as a function of x_{Et}: (◇) Data by Lai et al, 2014;[44] (□) data by Arce et al, 1996; (△) data by Yang and Wang, 2002;[52] (○) data by Kamihama et al, 2012.[53] The empty symbols correspond to the residuals for the NRTL model, and the filled ones correspond to the residuals for the UNIQUAC model.

the sum of quadratic errors between the experimental value and the respective calculated value.

$$T = \sum_{i=0}^{n} F_i x_{Et}{}^{i} \tag{A6}$$

A first representation of the integral argument as a function of x_{Et} is presented in Figure A1a. From this plot, it is possible to identify that several experimental points are slightly shifted from the main decreasing trend, which suggests that they are probably inconsistent. A new plot, presented in Figure A1b, is obtained by rejecting those specific data. The integral is finally calculated by smoothing this set experimental data with a polynomial correlation with order 3 (eq A6 with $n = 3$), ensuring a coefficient of determination (R^2) over 0.99. The value of A^* obtained in this case is 0.7, which means that the experimental data used as reference in this work pass the area test. Following the same procedure for the set of rejected data, plotted in Figure A1c, the value of A^* is 18.3, thus confirming that, in the light of this test, those data are not thermodynamically consistent.

Point-to-Point Test. The point-to-point test proposed by Van Ness et al.[66] is a modeling capability test, which assesses whether an activity coefficient model can accurately reproduce the experimental data. For isobaric sets, the approving criteria correspond to the average relative deviations (AAD%) of T and y_{Et}. The experimental set passes this test if the AAD% value for T is lower than 1% and that for y_{Et} does not exceed 10%.[67] In this context, according to Table 7, the test is verified for the NRTL (AAD% T = 0.2% and AAD% y_{Et} = 1.24%) and UNIQUAC models (AAD% T = 0.2% and AAD% y_{Et} = 1.27%), which represent the reference data set with the same high accuracy. The AAD% values were calculated without taking into account the inconsistent data identified in the area test.

This test is completed with an analysis of the relative residuals (AD%) for T and y_{Et}, presented in Figure A2 as a function of x_{Et}. The data set can be considered as consistent since the residuals are randomly scattered about the zero line.[68] From these residual plots, one can also confirm that the quality of data fitting obtained with both models is equivalent. They are equally recommended for the estimation of thermodynamic properties of ethanol−water mixtures.

■ ASSOCIATED CONTENT

Supporting Information

The Supporting Information is available free of charge on the ACS Publications website at DOI: 10.1021/acs.jced.7b00770.

Computation of combined standard uncertainties (u_c) for the equilibrium variables (PDF)

■ AUTHOR INFORMATION

Corresponding Author

*Tel.: + 33 169 93 50 92. E-mail: martine.decloux@agroparistech.fr.

ORCID

Cristian Puentes: 0000-0001-7126-1193

Patrice Paricaud: 0000-0003-4028-7133

Funding

This work was funded by the ABIES Doctoral School (AgroParisTech, Université Paris-Saclay; doctoral contract 2014-7).

Notes

The authors declare no competing financial interest.

■ ACKNOWLEDGMENTS

This work was supported by the ABIES Doctoral School (AgroParisTech, Université Paris-Saclay) and was carried out within the framework of the RMT FIDELE (Réseau mixte technologique Produits fermentés et distillés). The authors would also like to thank Elodie Phan (Université Pierre et Marie Curie) and Xuefan Song (AgroParisTech, Université Paris-Saclay) for their technical help in the Labodest experiments. Finally, the authors are grateful to the UNGDA laboratory, particularly to Sydney Cohen, as well as Nicolas Descharles (AgroParisTech, Université Paris-Saclay) for the training provided for the use of the GC-FID instrument.

REFERENCES

(1) Rhodes, C. L. The Process Simulation Revolution: Thermophysical Property Needs and Concerns. *J. Chem. Eng. Data* **1996**, *41*, 947−950.

(2) Baburao, B.; Visco, D. P. Methodology for the Development of Thermodynamic Models Describing Substances that Exhibit Complex Association Interactions. *J. Chem. Eng. Data* **2011**, *56*, 1506−1525.

(3) Hsieh, C.-M.; Sandler, S. I.; Lin, S.-T. Improvements of COSMO-SAC for vapor−liquid and liquid−liquid equilibrium predictions. *Fluid Phase Equilib.* **2010**, *297*, 90−97.

(4) Kang, J. W.; Diky, V.; Chirico, R. D.; Magee, J. W.; Muzny, C. D.; Abdulagatov, I.; Kazakov, A. F.; Frenkel, M. Quality Assessment Algorithm for Vapor−Liquid Equilibrium Data. *J. Chem. Eng. Data* **2010**, *55*, 3631−3640.

(5) Valderrama, J. O.; Faúndez, C. A.; Toselli, L. A. Advances on modeling and simulation of alcoholic distillation. Part 1: Thermodynamic modeling. *Food Bioprod. Process.* **2012**, *90*, 819−831.

(6) Esteban-Decloux, M.; Deterre, S.; Kadir, S.; Giampaoli, P.; Albet, J.; Joulia, X.; Baudouin, O. Two industrial examples of coupling experiments and simulations for increasing quality and yield of distilled beverages. *Food Bioprod. Process.* **2014**, *92*, 343−354.

(7) Valderrama, J. O.; Toselli, L. A.; Faúndez, C. A. Advances on modeling and simulation of alcoholic distillation. Part 2: Process simulation. *Food Bioprod. Process.* **2012**, *90*, 832−840.

(8) Gaiser, M.; Bell, G. M.; Lim, A. W.; Roberts, N. A.; Faraday, D. B. F.; Schulz, R. A.; Grob, R. Computer simulation of a continuous whisky still. *J. Food Eng.* **2002**, *51*, 27−31.

(9) Decloux, M.; Coustel, J. Simulation of a neutral spirit production plant using beer distillation. *Int. Sugar J.* **2005**, *107−1283*, 628−643.

(10) Batista, F. R. M.; Meirelles, A. J. A. A Strategy for Controlling Acetaldehyde Content in an Industrial Plant of Bioethanol. *IFAC Proceed. Vol.* **2009**, *42−11*, 928−933.

(11) Batista, F. R. M.; Follegatti-Romero, L. A.; Bessa, L.C.B.A.; Meirelles, A. J. A. Computational simulation applied to the investigation of industrial plants for bioethanol distillation. *Comput. Chem. Eng.* **2012**, *46*, 1−16.

(12) Tgarguifa, A.; Abderafi, S.; Bounahmidi, T. Energetic optimization of Moroccan distillery using simulation and response surface methodology. *Renewable Sustainable Energy Rev.* **2017**, *76*, 415−425.

(13) Batista, F. R. M.; Meirelles, A. J. A. Computer simulation applied to studying continuous spirit distillation and product quality control. *Food Control* **2011**, *22*, 1592−1603.

(14) Bastidas, P.; Parra, J.; Gil, I.; Rodriguez, G. Alcohol distillation plant simulation: thermal and hydraulic studies. *Procedia Eng.* **2012**, *42*, 80−89.

(15) Coelho, T. C.; Souza, O.; Sellin, N.; Medeiros, S. H. W.; Marangoni, C. Analysis of the reflux ratio on the batch distillation of bioethanol obtained from lignocellulosic residue. *Procedia Eng.* **2012**, *42*, 131−139.

(16) Osorio, D.; Pérez-Correa, R.; Belancic, A.; Agosin, E. Rigorous dynamic modeling and simulation of wine distillations. *Food Control* **2004**, *15*, 515−521.

(17) Carvallo, J.; Labbe, M.; Perez-Correa, J. R.; Zaror, C.; Wisniak, J. Modelling methanol recovery in wine distillation stills with packing columns. *Food Control* **2011**, *22*, 1322−1332.

(18) Scanavini, H. F. A.; Ceriani, R.; Cassini, C. E. B.; Souza, E. L. R.; Maugeri-Falco, F.; Meirelles, A. J. A. Cachaça Production in a Lab-Scale Alembic: Modeling and Computational Simulation. *J. Food Process Eng.* **2010**, *33*, 226−252.

(19) Scanavini, H. F. A.; Ceriani, R.; Meirelles, A. J. A. Cachaça Distillation Investigated on the Basis of Model Systems. *Braz. J. Chem. Eng.* **2012**, *29−02*, 429−440.

(20) Sacher, J.; García-Llobodanin, L.; López, F.; Segura, H.; Pérez-Correa, J. R. Dynamic modeling and simulation of an alembic pear wine distillation. *Food Bioprod. Process.* **2013**, *91*, 447−456.

(21) Maarse, H.; Van Den Berg, F. Flavour of distilled beverages. In *Understanding of natural flavors*; Piggott, J. R.; Paterson, A., Eds.; Springer Science+Business Media Dordetch: London, 1994.

(22) Suomalainen, H.; Lehtonen, M. The production of Aroma Compounds by Yeast. *J. Inst. Brew.* **1979**, *85*, 149−156.

(23) Ebeler, S. E. Analytical Chemistry: Unlocking the Secrets of Wine. *Food Rev. Int.* **2001**, *17*, 45−64.

(24) Ortega, C.; López, R.; Cacho, J.; Ferreira, V. Fast analysis of important wine volatile compounds: Development and validation of a new method based on gas chromatographic−flame ionisation detection analysis of dichloromethane microextracts. *J. Chromatog. A* **2001**, *923*, 205−214.

(25) Martí, M. P.; Mestres, M.; Sala, C.; Busto, O.; Guasch, J. Solid-Phase Microextraction and Gas Chromatography Olfactometry Analysis of Successively Diluted Samples. A New Approach of the Aroma Extract Dilution Analysis Applied to the Characterization of Wine Aroma. *J. Agric. Food Chem.* **2003**, *51*, 7861−7865.

(26) Jiang, B.; Zhang, Z. Volatile Compounds of Young Wines from Cabernet Sauvignon, Cabernet Gernischet and Chardonnay Varieties Grown in the Loess Plateau Region of China. *Molecules* **2010**, *15*, 9184.

(27) Nykänien, L.; Suomalainen, H. *Aroma of Beer, Wine and Distilled Alcoholic Beverages*; D. Reidel Publishing Company: Dordrecht, Germany, 1983.

(28) Apostolopoulou, A. A.; Flouros, A. I.; Demertzis, P. G.; Akrida-Demertzi, K. Differences in concentration of principal volatile constituents in traditional Greek distillates. *Food Control* **2005**, *16*, 157−164.

(29) Ledauphin, J.; Le Milbeau, C.; Barillier, D.; Hennequin, D. Differences in the Volatile Compositions of French Labeled Brandies (Armagnac, Calvados, Cognac, and Mirabelle) Using GC-MS and PLS-DA. *J. Agric. Food Chem.* **2010**, *58*, 7782−7793.

(30) Bankfort, C. W.; Ward, R. E. *The Oxford Handbook of Food Fermentations*; Oxford University Press: Oxford, 2014.

(31) Decloux, M. *Simulation of Cognac Distillation. Confidential Document*; AgroParisTech: Paris, 2009.

(32) Weidlich, U.; Gmehling, J. A modified UNIFAC model. 1. Prediction of VLE, h^E, and Gamma at Infinite Dilution. *Ind. Eng. Chem. Res.* **1987**, *26*, 1372−1381.

(33) Gmehling, J.; Li, J.; Schiller, M. A modified UNIFAC model. 2. Present parameter matrix and results for different thermodynamic properties. *Ind. Eng. Chem. Res.* **1993**, *32*, 178−193.

(34) Cantagrel, R.; Lurton, L.; Vidal, J.-P.; Galy, B. La distillation charentaise pour l'obtention des eaux-de-vie de Cognac. In 1er Symposium International Sur Les Eaux-De-Vie Traditionnelles d'Origine Viticole; Bordeaux, France, 1990.

(35) Peña-Tejedor, S.; Murga, R.; Sanz, M. T.; Beltrán, S. Vapor−liquid equilibria and excess volumes of the binary systems ethanol + ethyl lactate, isopropanol + isopropyl lactate and n-butanol + n-butyl lactate at 101.325 kPa. *Fluid Phase Equilib.* **2005**, *230*, 197−203.

(36) Vu, D. T.; Lira, C. T.; Asthana, N. S.; Kolah, A. K.; Miller, D. J. Vapor−Liquid Equilibria in the Systems Ethyl Lactate + Ethanol and Ethyl Lactate + Water. *J. Chem. Eng. Data* **2006**, *51*, 1220−1225.

(37) Delgado, P.; Sanz, M. T.; Beltrán, S. Isobaric vapor−liquid equilibria for the quaternary reactive system: Ethanol + water + ethyl lactate + lactic acid at 101.33 kPa. *Fluid Phase Equilib.* **2007**, *255*, 17−23.

(38) Bertrand, A. Armagnac and Wine-Spirits. In *Fermented Beverage Production*; Lea, A. G. H.; Piggott, J. R., Eds.; Kluwer Academic/ Plenum Publishers: New York, 2003.

(39) Gillespie, D. T. C. Vapor-Liquid Equilibrium Still for Miscible Liquids. *Ind. Eng. Chem., Anal. Ed.* **1946**, *18*, 575−577.

(40) Christensen, S. P. Measurement of dilute mixture vapor−liquid equilibrium data for aqueous solutions of methanol and ethanol with a recirculating still. *Fluid Phase Equilib.* **1998**, *150−151*, 763−773.

(41) Rall, J. D.; Mühlbauer, A. L. *Phase Equilibria: Measurement and Computation*; Taylor & Francis: WA, 1998.

(42) Athès, V.; Paricaud, P.; Ellaite, M.; Souchon, I.; Fürst, W. Vapour−liquid equilibria of aroma compounds in hydroalcoholic solutions: Measurements with a recirculation method and modelling with the NRTL and COSMO-SAC approaches. *Fluid Phase Equilib.* **2008**, *265*, 139−154.

(43) Deterre, S.; Albet, J.; Joulia, X.; Baudouin, O.; Giampaoli, P.; Decloux, M.; Athès, V. Vapor−Liquid Equilibria Measurements of Bitter

Orange Aroma Compounds Highly Diluted in Boiling Hydro-Alcoholic Solutions at 101.3 kPa. *J. Chem. Eng. Data* **2012**, *57*, 3344−3356.
(44) Lai, H.-S.; Lin, Y.-F.; Tu, C.-H. Isobaric (vapor + liquid) equilibria for the ternary system of (ethanol + water + 1,3-propanediol) and three constituent binary systems at P = 101.3 kPa. *J. Chem. Thermodyn.* **2014**, *68*, 13−19.
(45) Faúndez, C. A.; Valderrama, J. O. Phase equilibrium modeling in binary mixtures found in wine and must distillation. *J. Food Eng.* **2004**, *65*, 577−583.
(46) Faúndez, C. A.; Alvarez, V. H.; Valderrama, J. O. Predictive models to describe VLE in ternary mixtures water + ethanol + congener for wine distillation. *Thermochim. Acta* **2006**, *450*, 110−117.
(47) Faúndez, C. A.; Valderrama, J. O. Activity Coefficient Models to Describe Vapor-Liquid Equilibrium in Ternary Hydro-Alcoholic Solutions. *Chin. J. Chem. Eng.* **2009**, *17*, 259−267.
(48) Nala, M.; Auger, E.; Gedik, I.; Ferrando, N.; Dicko, M.; Paricaud, P.; Volle, F.; Passarello, J. P.; de Hemptinne, J.-C.; Tobaly, P.; et al. Vapour−liquid equilibrium (VLE) for the systems furan + n-hexane and furan + toluene. Measurements, data treatment and modeling using molecular models. *Fluid Phase Equilib.* **2013**, *337*, 234−245.
(49) Dias, T.P.V.B.; Fonseca, L.A.A.P.; Ruiz, M. C.; Batista, F. R. M.; Batista, E. A. C.; Meirelles, A. J. A. Vapor−Liquid Equilibrium of Mixtures Containing the Following Higher Alcohols: 2-Propanol, 2-Methyl-1-propanol, and 3-Methyl-1-butanol. *J. Chem. Eng. Data* **2014**, *59*, 659−665.
(50) Kadir, S. *Optimisation du procédé de production d'Alcool surfin*. Ph.D. Thesis, AgroParisTech, Paris, 2009.
(51) Arce, A.; Martinez-Ageitos, J.; Soto, A. VLE for water + ethanol + 1-octanol mixtures. Experimental measurements and correlations. *Fluid Phase Equilib.* **1996**, *122*, 117−129.
(52) Yang, B.; Wang, H. Vapor-Liquid Equilibrium for Mixtures of Water, Alcohols, and Ethers. *J. Chem. Eng. Data* **2002**, *47*, 1324−1329.
(53) Kamihama, N.; Matsuda, H.; Kurihara, K.; Tochigi, K.; Oba, S. Isobaric Vapor−Liquid Equilibria for Ethanol + Water + Ethylene Glycol and Its Constituent Three Binary Systems. *J. Chem. Eng. Data* **2012**, *57*, 339−344.
(54) Taylor, B. N.; Kuyatt, C. E. *Guidelines for Evaluating and Expressing the Uncertainty of NIST Measurement Results*; NIST Technical Note 1297; NIST, Gaithersburg, 1994.
(55) Prausnitz, J. M.; Lichtenthaler, R. N.; de Azevedo, E. G. *Molecular Thermodynamics of Fluid-Phase Equilibria*; Prentice Hall PTR: NJ, 1999.
(56) Rios, K. *Lecture Notes on Chemical Thermodynamics*; National University of Colombia: Bogota, 2009.
(57) Dahm, K. D.; Visco, D. P. *Fundamentals of Chemical Engineering Thermodynamics*; Cencage Learning: Stamford, 2015.
(58) Letcher, T. M. *Developments and Applications in Solubility*; The Royal Society of Chemistry: Cambridge, 2007.
(59) Coquelet, C.; Laurens, S.; Richon, D. Measurement through a Gas Stripping Technique of Henry's Law Constants and Infinite Dilution Activity Coefficients of Propyl Mercaptan, Butyl Mercaptan, and Dimethyl Sulfide in Methyldiethanolamine (1) + Water (2) with w_1 = 0.25 and 0.35. *J. Chem. Eng. Data* **2008**, *53*, 2540−2543.
(60) Vetere, A. The Riedel equation. *Ind. Eng. Chem. Res.* **1991**, *30*, 2487−2492.
(61) Li, J.; Paricaud, P. Application of the Conduct-like Screening Models for Real Solvent and Segment Activity Coefficient for the Predictions of Partition Coefficients and Vapor−Liquid and Liquid−Liquid Equilibria of Bio-oil-Related Mixtures. *Energy Fuels* **2012**, *26*, 3756−3768.
(62) Wilson, G. M. Vapor-Liquid Equilibrium. XI. A New Expression for the Excess Free Energy of Mixing. *J. Am. Chem. Soc.* **1964**, *86*, 127−130.
(63) Renon, H.; Prausnitz, J. M. Local compositions in thermodynamic excess functions for liquid mixtures. *AIChE J.* **1968**, *14*, 135−144.
(64) Lasdon, L. S.; Fox, R. L.; Ratner, M. W. Nonlinear optimization using the generalized reduced gradient method. *R.A.I.R.O. Recherche opérationnelle* **1974**, *8*, 73−103.
(65) Kurihara, K.; Egawa, Y.; Kojima, K. Evaluation of thermodynamic consistency of isobaric and isothermal binary vapor−liquid equilibrium data using the PAI test. *Fluid Phase Equilib.* **2004**, *219*, 75−85.
(66) Van Ness, H.; Byer, S.; Gibbs, R. Vapor−liquid equilibrium: Part 1. An appraisal of Data Reduction Methods. *AIChE J.* **1973**, *19* (2), 238−244.
(67) Faundez, C.; Quiero, F.; Valderrama, J. Thermodynamic consistency test for binary gas + wáter equilibrium data at low and high pressures. *Chin. J. Chem. Eng.* **2013**, *21* (10), 1172−1181.
(68) Wisniak, J.; Apelblat, A.; Segura, H. An assessment of thermodynamic consistency tests for vapor−liquid equilibrium data. *Phys. Chem. Liq.* **1997**, *35* (1), 1−58.
(69) Larkin, J. Thermodynamic properties of aqueous non-electrolyte mixtures. I. Excess enthalpy for water + ethanol at 298.15 to 383.15 K. *J. Chem. Thermodyn.* **1975**, *7*, 137−148.
(70) Riddick, J. A.; Bunger, W. B.; Sakano, T. K. *Organic Solvents Physical Properties and Methods of Purification*; Wiley: New York, 1986.
(71) Abrams, D. S.; Prausnitz, J. M. Statistical thermodynamics of liquid mixtures: A new expression for the excess Gibbs energy of partly or completely miscible systems. *AIChE J.* **1975**, *21*, 116−128.
(72) Anderson, T. F.; Prausnitz, J. M. Application of the UNIQUAC Equation to Calculation of Multicomponent Phase Equilibria. 1. Vapor-Liquid Equilibria. *Ind. Eng. Chem. Process Des. Dev.* **1978**, *17*, 552−561.

SUPPORTING INFORMATION

Vapor–liquid equilibrium (VLE) of ethyl lactate highly diluted in ethanol–water mixtures at 101.3 kPa. Experimental measurements and thermodynamic modeling using semi–empirical models

Cristian Puentes[a], Xavier Joulia[b], Patrice Paricaud[c], Pierre Giampaoli[a], Violaine Athès[d], Martine Esteban-Decloux[a]*

[a] Unité Mixte de Recherche Ingénierie Procédés Aliments, AgroParisTech, INRA, Université Paris-Saclay, F-91300 Massy, France.
[b] Laboratoire de Génie Chimique, Université de Toulouse INPT-ENSIACET, CNRS, F-31030 Toulouse, France.
[c] Unité de Chimie et Procédés, ENSTA ParisTech, Université Paris-Saclay, F-91762 Palaiseau, France.
[d] Unité Mixte de Recherche Génie et Microbiologie des Procédés Alimentaires, AgroParisTech, INRA, Université Paris-Saclay, F-78850 Thiverval-Grignon, France.

Corresponding author
* Tel: + 33 169 93 50 92. E-mail: martine.decloux@agroparistech.fr.

Computation of combined standard uncertainties (u_c) for the equilibrium variables

The combined standard uncertainty represents the estimated standard deviation of an indirect measurement and is calculated as the positive square root of the estimated variance u_c^2. The combined expanded uncertainty, U_c, is obtained by multiplying u_c by the selected coverage factor k.[54]

Mass compositions

Ethyl Lactate
Uncertainty associated with the mass measurements as well as the three replicates of sample injections during the chromatographic analysis:

$$u_c^2(z_{mEL}) = \sum_{i=1} \left(\frac{\partial z_{mEL}}{\partial m_i}\right)^2 u^2(m_i) + \left(\frac{\partial z_{mEL}}{\partial R_{A_{EL\text{-}IS}}}\right)^2 u^2\left(R_{A_{EL\text{-}IS}}\right)$$

Relationship between mass composition, area ratio of Ethyl Lactate - internal standard peaks and reagents masses:

$$z_{mEL} = \left(\frac{R_{A_{EL\text{-}IS}}}{k_{Calibration}}\right)\left(\frac{m_{IS\text{-}SM_0}}{m_{SM\text{-}IS_0}}\frac{m_{SM\text{-}IS_f}}{m_{Sample}}\right)$$

Hence:

$$u_c^2(z_{mEL}) = \left(\frac{R_{A_{EL\text{-}IS}}}{k_{Calibration}}\right)^2 \left[\left(\frac{1}{m_{SM\text{-}IS_0}}\frac{m_{SM\text{-}IS_f}}{m_{Sample}}\right)^2 u^2\left(m_{IS\text{-}SM_0}\right) + \left(\frac{m_{SM\text{-}IS_0}}{m_{SM\text{-}IS_0}^2}\frac{m_{SM\text{-}IS_f}}{m_{Sample}}\right)^2 u^2\left(m_{SM\text{-}IS_0}\right) + \left(\frac{m_{IS\text{-}SM_0}}{m_{SM\text{-}IS_0}}\frac{1}{m_{Sample}}\right)^2 u^2\left(m_{SM\text{-}IS}\right) + \left(\frac{m_{IS\text{-}SM_0}}{m_{SM\text{-}IS_0}}\frac{m_{SM\text{-}IS_f}}{m_{Sample}^2}\right)^2 u^2\left(m_{Sample}\right)\right]$$
$$+ \left(\frac{1}{k_{Calibration}}\right)^2 \left(\frac{m_{IE\text{-}SM_0}}{m_{SM\text{-}IE_0}}\frac{m_{SM\text{-}IE}}{m_{Sample}}\right)^2 u^2\left(R_{A_{EL\text{-}IS}}\right)$$

Here:

$$u(m_{IS\text{-}SM_0}) = u(m_{SM\text{-}IS_f}) = u(m_{Sample}) = u(m_1) = 0.00006 \text{ g}$$
$$u(m_{SM\text{-}IS_0}) = u(m_2) = 0.006 \text{ g}$$

Therefore:

$$u_c^2(z_{mEL}) = \left(\frac{R_{A_{EL\text{-}IS}}}{k_{Calibration}}\right)^2 \left[\left(\frac{1}{m_{SM\text{-}IS_0}}\frac{m_{SM\text{-}IS_f}}{m_{Sample}}\right)^2 + \left(\frac{m_{IS\text{-}SM_0}}{m_{SM\text{-}IS_0}}\frac{1}{m_{Sample}}\right)^2 + \left(\frac{m_{IS\text{-}SM_0}}{m_{SM\text{-}IS_0}}\frac{m_{SM\text{-}IS_f}}{m_{Sample}^2}\right)^2\right] u^2(m_1)$$
$$+ \left(\frac{R_{A_{EL\text{-}IS}}}{k_{Calibration}}\right)^2 \left(\frac{m_{SM\text{-}IS_0}}{m_{SM\text{-}IS_0}^2}\frac{m_{SM\text{-}IS_f}}{m_{Sample}}\right)^2 u^2(m_2)$$
$$+ \left(\frac{1}{k_{Calibration}}\right)^2 \left(\frac{m_{IS\text{-}SM_0}}{m_{SM\text{-}IS_0}}\frac{m_{SM\text{-}IS_f}}{m_{Sample}}\right)^2 u^2(R_{A_{EL\text{-}IS}})$$

Ethanol

Uncertainty associated with the temperature and pressure measurements in the equilibrium experiments:

$$u_c^2(z_{mEt}) = \left(\frac{\partial z_{mEt}}{\partial T}\right)^2 u^2(T) + \left(\frac{\partial z_{mEt}}{\partial P}\right)^2 u^2(P) = \left(\frac{\partial z_{mEt}}{\partial z_{Et}}\right)^2 \left[\left(\frac{\partial z_{Et}}{\partial T}\right)^2 u^2(T) + \left(\frac{\partial z_{Et}}{\partial P}\right)^2 u^2(P)\right]$$

Relationship between composition, temperature and pressure given by the equilibrium relation for the binary system Ethanol - Water the, namely:

$$y_{Et}P = \gamma_{Et}(T, \boldsymbol{x}) x_{Et} P_{Et}^0(T)$$

Where:

- $\gamma_{Et}(T, \boldsymbol{x})$ determined with NRTL model, Table 3, Eq 3.1.
- $P_{Et}^0(T)$ calculated by means of the Riedel equation, Eq 8 with the coefficients given in Table 2.

Therefore, for the liquid phase:

$$x_{Et} = \frac{y_{Et}P}{\gamma_{Et}P_{Et}^0}$$

$$u_c^2(x_{mEt}) = \left[\frac{MM_{Et}MM_W}{(MM_{Et}x_{Et} - MM_W x_{Et} + MM_W)^2}\right]^2 \left[\left(\frac{y_{Et}P\gamma_{Et}}{\gamma_{Et}^2 P_{Et}^{02}}\right)^2 \left(P_{Et}^{0L}\frac{\partial \ln \gamma_{Et}}{\partial T} + \frac{\partial P_{Et}^0}{\partial T}\right)^2 u^2(T) + \left(\frac{y_{Et}}{\gamma_{Et}P_{Et}^0}\right)^2 u^2(P)\right]$$

And for the vapor phase:

$$y_{Et} = \frac{x_{Et}\gamma_{Et}P_{Et}^0}{P}$$

$$u_c^2(y_{mEt}) = \left[\frac{MM_{Et}MM_W}{(MM_{Et}y_{Et} - MM_W y_{Et} + MM_W)^2}\right]^2 \left[\left(\frac{x_{Et}\gamma_{Et}}{P}\right)^2 \left(P_{Et}^0\frac{\partial \ln \gamma_{Et}}{\partial T} + \frac{\partial P_{Et}^0}{\partial T}\right)^2 u^2(T) + \left(\frac{x_{Et}\gamma_{Et}P_{Et}^0}{P^2}\right)^2 u^2(P)\right]$$

$\frac{\partial P_{Et}^0(T)}{\partial T}$ and $\frac{\partial \ln \gamma_{Et}(T,x)}{\partial T}$ are obtained analytically. The final expressions are:

- $P_{Et}^0(T)$:

$$\frac{\partial P_{Et}^0(T)}{\partial T} = P_{Et}^0(T)\left(-\frac{B}{T^2} + \frac{C}{T} + EDT^{E-1}\right)$$

- $ln\,\gamma_{Et}(T, \boldsymbol{x})$: The function differentiated is the simplified version of the NRTL model for a binary system, that is,

$$ln\,\gamma_{Et}(T,\boldsymbol{x}) = x_W^2\left[\tau_{W\text{-}Et}\left(\frac{G_{W\text{-}Et}}{x_{Et} + x_W G_{W\text{-}Et}}\right)^2 + \frac{\tau_{Et\text{-}W}G_{Et\text{-}W}}{(x_W + x_{Et}G_{Et\text{-}W})^2}\right]$$

Hence:

$$\frac{\partial \ln \gamma_{Et}(T,x)}{\partial T} = x_W^2\left[\left(\frac{G_{W\text{-}Et}}{x_{Et} + x_W G_{W\text{-}Et}}\right)^2 \frac{\partial \tau_{W\text{-}Et}}{\partial T} + 2\tau_{W\text{-}Et}\left(\frac{G_{W\text{-}Et}}{x_{Et} + x_W G_{W\text{-}Et}}\right)\left(\frac{x_{Et}}{(x_{Et} + x_W G_{W\text{-}Et})^2}\frac{\partial G_{W\text{-}Et}}{\partial T}\right)\right]$$
$$+ x_W^2\left[\frac{\left(G_{Et\text{-}W}\frac{\partial \tau_{Et\text{-}W}}{\partial T} + \tau_{Et\text{-}W}\frac{\partial G_{Et\text{-}W}}{\partial T}\right)(x_W + x_{Et}G_{Et\text{-}W})^2 - 2\tau_{Et\text{-}W}x_{Et}G_{Et\text{-}W}(x_W + x_{Et}G_{Et\text{-}W})\frac{\partial G_{Et\text{-}W}}{\partial T}}{(x_W + x_{Et}G_{Et\text{-}W})^4}\right]$$

With:

$$\frac{\partial G_{Et\text{-}W}}{\partial T} = -c^0 exp(-c^0\tau_{Et\text{-}W})\frac{\partial \tau_{Et\text{-}W}}{\partial T}$$
$$\frac{\partial \tau_{Et\text{-}W}}{\partial T} = \frac{-R\left(A_{Et\text{-}W}^0 + 273.15A_{Et\text{-}W}^T\right)}{R^2T^2}$$
$$\frac{\partial G_{W\text{-}Et}}{\partial T} = -c^0 exp(-c^0\tau_{W\text{-}Et})\frac{\partial \tau_{W\text{-}Et}}{\partial T}$$

$$\frac{\partial \tau_{W\text{-}Et}}{\partial T} = \frac{\text{-}R\left(A^{0}_{W\text{-}Et} + 273.15A^{T}_{W\text{-}Et}\right)}{R^2T^2}$$

Water

Propagation of the combined uncertainties of the mass fractions of Ethyl Lactate and Ethanol:

$$u_c^2(z_{mW}) = \left(\frac{\partial z_{mW}}{\partial z_{mEL}}\right)^2 u_c^2(z_{mEL}) + \left(\frac{\partial z_{mW}}{\partial z_{mEt}}\right)^2 u_c^2(z_{mEt})$$

Relationship between z_{mW}, z_{mEL} and z_{mEt}

$$z_{mW} = 1 - z_{mEL} - z_{mEt}$$

Therefore:

$$u_c^2(z_{mW}) = u_c^2(z_{mEL}) + u_c^2(z_{mEt})$$

Mole compositions

Ethyl Lactate

Propagation of the standard uncertainties of the mass fractions of ethyl lactate, ethanol and water:

$$u_c^2(z_{EL}) = \left(\frac{\partial z_{EL}}{\partial z_{mEL}}\right)^2 u_c^2(z_{mEL}) + \left(\frac{\partial z_{EL}}{\partial z_{mEt}}\right)^2 u_c^2(z_{mEt}) + \left(\frac{\partial z_{EL}}{\partial z_{mW}}\right)^2 u_c^2(z_{mW})$$

Relationship between z_{EL}, z_{mEL}, z_{mEt} and z_{mW} given by:

$$z_{EL} = \frac{\frac{z_{mEL}}{MM_{EL}}}{\frac{z_{mEL}}{MM_{EL}} + \frac{z_{mEt}}{MM_{Et}} + \frac{z_{mW}}{MM_{W}}} = \frac{z_{mEL}MM_{EL}MM_{Et}MM_{W}}{z_{mEL}MM_{Et}MM_{W} + z_{mEt}MM_{EL}MM_{W} + z_{mW}MM_{EL}MM_{Et}}$$

Resulting expression:

$$\boldsymbol{u_c^2(z_{EL}) = \frac{\left(MM_{EL}MM_{Et}MM_{W}\left(z_{mEt}MM_{EL}MM_{W} + z_{mW}MM_{EL}MM_{Et}\right)\right)^2 u_c^2(z_{mEL}) + \left(z_{mEL}MM_{EL}^2MM_{Et}MM_{W}^2\right)^2 u_c^2(z_{mEt}) + \left(z_{mEL}MM_{EL}^2MM_{Et}^2MM_{W}\right)^2 u_c^2(z_{mW})}{\left[\left(z_{mEL}MM_{Et}MM_{W} + z_{mEt}MM_{EL}MM_{W} + z_{mW}MM_{EL}MM_{Et}\right)^2\right]^2}}$$

Ethanol

Analogous calculation to that for Ethyl Lactate:

$$u_c^2(z_{Et}) = \left(\frac{\partial z_{Et}}{\partial z_{mEL}}\right)^2 u_c^2(z_{mEL}) + \left(\frac{\partial z_{Et}}{\partial z_{mEt}}\right)^2 u_c^2(z_{mEt}) + \left(\frac{\partial z_{Et}}{\partial z_{mW}}\right)^2 u_c^2(z_{mW})$$

$$\boldsymbol{u_c^2(z_{EL}) = \frac{\left(MM_{EL}MM_{Et}MM_{W}\left(z_{mEL}MM_{Et}MM_{W} + z_{mW}MM_{EL}MM_{Et}\right)\right)^2 u_c^2(z_{mEt}) + \left(z_{mEt}MM_{EL}MM_{Et}^2MM_{W}^2\right)^2 u_c^2(z_{mEL}) + \left(z_{mEt}MM_{EL}^2MM_{Et}^2MM_{W}\right)^2 u_c^2(z_{mW})}{\left[\left(z_{mEL}MM_{Et}MM_{W} + z_{mEt}MM_{EL}MM_{W} + z_{mW}MM_{EL}MM_{Et}\right)^2\right]^2}}$$

Water

Analogous calculation to that for water mass fraction:

$$u_c^2(z_W) = \left(\frac{\partial z_W}{\partial z_{EL}}\right)^2 u_c^2(z_{EL}) + \left(\frac{\partial z_W}{\partial z_{Et}}\right)^2 u_c^2(z_{Et})$$

$$u_c^2(z_W) = u_c^2(z_{EL}) + u_c^2(z_{Et})$$

Activity coefficient of Ethyl Lactate

$$\gamma^{\infty}_{EL}(T, \boldsymbol{x_s}) = \frac{y_{EL}P}{x_{EL}P^{0}_{EL}(T)}$$

$$u_c^2\left(\gamma^{\infty}_{EL}\right) = \left(\frac{\partial \gamma^{\infty}_{EL}}{\partial y_{EL}}\right)^2 u_c^2(y_{EL}) + \left(\frac{\partial \gamma^{\infty}_{EL}}{\partial x_{EL}}\right)^2 u_c^2(x_{EL}) + \left(\frac{\partial \gamma^{\infty}_{EL}}{\partial P^{0}_{EL}}\right)^2 \left(\frac{\partial P^{0}_{EL}}{\partial T}\right)^2 u^2(T) + \left(\frac{\partial \gamma^{\infty}_{EL}}{\partial P}\right)^2 u^2(P)$$

$$\boldsymbol{u_c^2\left(\gamma^{\infty}_{EL}\right) = \left(\frac{P}{x_{EL}P^{0}_{EL}}\right)^2 u_c^2(y_{EL}) + \left(\frac{y_{EL}P}{x_{EL}^2P^{0}_{EL}}\right)^2 u_c^2(x_{EL}) + \left(\frac{y_{EL}P}{x_{EL}P^{0}_{EL}{}^2}\right)^2 \left[P^{0}_{Et}(T)\left(\text{-}\frac{B}{T^2} + \frac{C}{T} + EDT^{E\text{-}1}\right)\right]^2 u^2(T) + \left(\frac{y_{EL}}{x_{EL}P^{0}_{EL}(T)}\right)^2 u^2(P)}$$

Henry constant of Ethyl lactate

$$\mathcal{H}_{EL}(T,\boldsymbol{x_s})=\gamma^{\infty}_{EL}(T,\boldsymbol{x_s})P^{O}_{EL}(T)$$

$$u_c^2(\mathcal{H}_{EL})=\left(\frac{\partial \mathcal{H}_{EL}}{\partial \gamma^{\infty}_{EL}}\right)^2 u_c^2(\gamma^{\infty}_{EL})+\left(\frac{\partial \mathcal{H}_{EL}}{\partial P^{O}_{EL}}\right)^2\left(\frac{\partial P^{O}_{EL}}{\partial T}\right)^2 u^2(T)$$

$$\boldsymbol{u_c^2(\mathcal{H}_{EL})=P^{O}_{EL}{}^2\,u_c^2(\gamma^{\infty}_{EL})+\gamma^{\infty}_{EL}{}^2\left[P^{O}_{EL}\left(-\frac{B}{T^2}+\frac{C}{T}+EDT^{E-1}\right)\right]^2 u^2(T)}$$

Volatility of Ethyl lactate

Absolute volatility

$$K_{EL}=\frac{y_{EL}}{x_{EL}}$$

$$u_c^2(K_{EL})=\left(\frac{\partial K_{EL}}{\partial y_{EL}}\right)^2 u_c^2(y_{EL})+\left(\frac{\partial K_{EL}}{\partial x_{EL}}\right)^2 u_c^2(x_{EL})$$

$$\boldsymbol{u_c^2(K_{EL})=\left(\frac{1}{x_{EL}}\right)^2 u_c^2(y_{EL})+\left(\frac{y_{EL}}{x_{EL}^2}\right)^2 u_c^2(x_{EL})}$$

Relative volatility with respect to ethanol

$$\alpha_{EL/Et}=\frac{K_{EL}}{K_{Et}}=\frac{y_{EL}/x_{EL}}{y_{Et}/x_{Et}}=\frac{y_{mEL}/x_{mEL}}{y_{mEt}/x_{mEt}}=\frac{y_{mEL}x_{mEt}}{y_{mEt}x_{mEL}}$$

$$u_c^2(\alpha_{EL/Et})=\left(\frac{\partial \alpha_{EL/Et}}{\partial y_{mEL}}\right)^2 u_c^2(y_{mEL})+\left(\frac{\partial \alpha_{EL/Et}}{\partial x_{mEL}}\right)^2 u_c^2(x_{mEL})+\left(\frac{\partial \alpha_{EL/Et}}{\partial y_{mEt}}\right)^2 u_c^2(y_{mEt})+\left(\frac{\partial \alpha_{EL/Et}}{\partial x_{mEt}}\right)^2 u_c^2(x_{mEt})$$

$$\boldsymbol{u_c^2(\alpha_{EL/Et})=\left(\frac{x_{mEt}}{y_{mEt}x_{mEL}}\right)^2 u_c^2(y_{mEL})+\left(\frac{y_{mEL}x_{mEt}}{y_{mEt}x_{mEL}^2}\right)^2 u_c^2(x_{mEL})+\left(\frac{y_{mEL}x_{mEt}}{y_{mEt}^2x_{mEL}}\right)^2 u_c^2(y_{mEt})+\left(\frac{y_{mEL}}{y_{mEt}x_{mEL}}\right)^2 u_c^2(x_{mEt})}$$